NASA Technical Memorandum 100508

AN ANALYTICAL STUDY OF THE EFFECTS OF TRANSVERSE SHEAR DEFORMATION AND ANISOTROPY ON BUCKLING LOADS OF LAMINATED CYLINDERS

DAWN C. JEGLEY

OCTOBER 1987

(NASA-TM-100508) AN ANALYTICAL STUDY OF THE EFFECTS OF TRANSVERSE SHEAR DEFORMATION AND ANISOTROPY ON BUCKLING LOADS OF LAMINATED CYLINDERS M.S. Thesis - George Washington Univ. (NASA) 90 p Avail: NTIS HC A05/MF G3/24 N88-13387 Unclas 0106520

National Aeronautics and
Space Administration

Langley Research Center
Hampton, Virginia 23665

ABSTRACT

Buckling loads of thick-walled orthotropic and anisotropic simply supported circular cylinders are predicted using a higher-order transverse-shear deformation theory. A comparison of buckling loads predicted by the conventional first-order transverse-shear deformation theory and the higher-order theory shows that the additional allowance for transverse shear deformation has a negligible effect on the predicted buckling loads of medium-thickness metallic isotropic cylinders. However, the higher-order theory predicts buckling loads which are significantly lower than those predicted by the first-order transverse-shear deformation theory for certain short, thick-walled cylinders which have low through-the-thickness shear moduli. A parametric study of the effects of ply orientation on the buckling load of axially compressed cylinders indicates that laminates containing 45-degree plies are most sensitive to transverse-shear deformation effects. Interaction curves for buckling loads of cylinders subjected to axial compressive and external pressure loadings indicate that buckling loads due to external pressure loadings are as sensitive to transverse-shear deformation effects as buckling loads due to axial compressive loadings. The effects of anisotropy are important over a much wider range of cylinder geometries than the effects of transverse shear deformation. Neglecting either anisotropic effects or transverse-shear deformation effects leads to non-conservative errors in predicted buckling loads.

TABLE OF CONTENTS

TABLE OF CONTENTS ii

NOMENCLATURE iii

CHAPTER

I. INTRODUCTION 1

1.1 General 1
1.2 Objectives and Scope 2
1.3 Brief Review of Pertinent Literature 3

II. ANALYSIS APPROACH 8

2.1 Isotropic and Orthotropic Analysis 8
2.2 Anisotropic Analysis 24
2.3 Shear Correction Factors 28
2.4 Sensitivity to Anisotropy 29

III. RESULTS AND DISCUSSION 30

3.1 Axial Compression 30
3.2 Combined Loads 47

IV. CONCLUDING REMARKS AND RECOMMENDATIONS FOR FUTURE RESEARCH 49

4.1 Summary 49
4.2 Conclusions 50
4.3 Recommendations for Future Research 54

APPENDIX A 56

REFERENCES 61

FIGURES 64

NOMENCLATURE

$[B_1],[B_2]$	geometric stiffness matricies of orthotropic cylinder for axial compressive loading and external presssure loadings, respectively (one axial mode shape)
$[B_1]_A,[B_2]_A$	geometric stiffness matricies of anisotropic cylinder for axial compressive and external pressure loadings, respectively (several axial mode shapes)
$[C_{ij}]$	orthotropic material stiffness matrix
C_{16},C_{26}	anisotropic material stiffnesses
D	bending stiffness of isotropic wall
D_{11},D_{22}	bending stiffnesses of laminated shell
D_{16},D_{26}	anisotropic laminate stiffnesses
E	Young's modulus of isotropic material
E_l,E_t,E_z	Young's moduli of unidirectional zero-degree laminate in longitudinal, transverse and thickness directions, respectively
$f(m_i,m_j)$	block matrix of material stiffness matrix of anisotropic cylinder which is dependent upon axial wave numbers m_i and m_j
G	Shear modulus of isotropic material
G_{lt},G_{lz},G_{tz}	Shear moduli of zero-degree laminate
$G_{x\theta},G_{xz},G_{z\theta}$	Shear moduli of laminated cylinder wall
k_x	nondimensionalized buckling load of cylinder: $k_x=N_xL^2/D\pi^2$ for isotropic walls and $k_x=N_xL^2/(\sqrt{D_{11}D_{22}}\ \pi^2)$ for laminated

	walls
$\bar{k}_x$	nondimensionalized approximate buckling load of anisotropic cylinder
$[K]$	stiffness matrix of orthotropic cylinder (one axial mode shape)
$[K]_o$	stiffness matrix of orthotropic cylinder (several axial mode shapes)
$[K]_a$	anisotropic terms of stiffness matrix $[K]_{ANISO}$
$[K]_{ANISO}$	stiffness matrix of anisotropic cylinder
L	length of cylinder
m,n	number of half-waves in axial direction and number of waves in circumferential direction of buckled cylinder
N	number of terms summed in Fourier series for anisotropic analysis
N_x, N_θ	resultant normal forces at buckling
P	external pressure loading
R	radius of cylinder measured to wall centerline
s	nondimensional parameter for describing isotropic cylinders: $s=D\pi^2/GtL^2$
t	wall thickness of cylinder
U,V,W	cylinder displacements in axial, circumferential and radial directions, respectively (independent of x, z and θ)
u,v,w	cylinder displacements in axial, circumferential and radial directions, respectively (functions of x, z and θ)

$\bar{u},\bar{v},\bar{w}$	small changes in cylinder displacements which occur at buckling in the axial, circumferential and radial directions, respectively
$\tilde{u},\tilde{v},\tilde{w}$	cylinder displacements in axial, circumferential and radial directions, respectively (includes prebuckling displacements and small changes which occur at buckling)
x,z	cylinder axes in axial and radial directions
{x}	vector of displacements
Z	nondimensional parameter: $Z=L^2\sqrt{12(1-\mu^2)}/Rt$ for isotropic walls and $Z=L^2\sqrt{12(1-\mu_{12}\mu_{21})}/Rt$ for laminates
$\alpha,\beta,\Delta,\eta,$ κ,ξ,ψ	components in stiffness matrix (see equations (8))
$\epsilon_x,\epsilon_\theta,\epsilon_z$	normal strains
λ	parameter which specifies if orthotropic terms are to be included or neglected (λ = 1 or 0, respectively)
μ	Poisson's ratio of isotropic material
μ_{12},μ_{21}	Poisson's ratios of laminate
Π	virtual work
Ω	eigenvalue of anisotropic problem
ρ	measure of sensitivity to anisotropy: $\rho=(\partial^2\Omega/\partial\lambda^2)/(\ 2\ \Omega\ )$
$\gamma_{x\theta},\gamma_{xz},\gamma_{\theta z}$	shear strains
θ	axis in circumferential direction
Θ	ply angle
$\sigma_x,\sigma_\theta,\sigma_z$	normal stresses

$\tau_{xz}, \tau_{x\theta}, \tau_{\theta z}$	shear stresses
δ	variation
ω	eigenvalue of orthotropic buckling problem

Superscripts and subscripts

o,a,l	constant, linear and trigonometric terms through the thickness
$()_{,x}$, $()_{,\theta}$, $()_{,z}$	differentiation with respect to x, θ, z, respectively
$[\ ]_{ns}$	laminate in which the bracketted quantity is repeated n times then made symmetric
$\{\ \}^t$	transpose of matrix $\{\ \}$

CHAPTER I

INTRODUCTION

1.1 General

Fiber reinforced composite materials have higher stiffness-to-weight and strength-to-weight ratios than metals so they provide a useful lightweight alternative to traditional materials in some structural components. Because of these higher specific strength and stiffness ratios, more efficient structural components can be built from composites than from metals for many aircraft applications. However, before composite materials can be used efficiently and safely, their limitations and failure modes must be understood. The limitations and weaknesses of composite structures are not always the same as those of metal ones. For example, transverse shear deformations have a more significant effect on the behavoir of laminated structures than on metal ones. This phenomenon can be more severe in structures made of composite materials than those made of homogeneous metallic materials because laminated composites are more flexible in the through-the-thickness direction. One structural response which is particularly sensitive to transverse-shear deformation effects is buckling. Current theories do not always adequately account for transverse-shear deformation effects in the buckling of thick-walled circular cylinders made of materials such as fiber reinforced composites. Not adequately accounting for transverse shearing may lead to non-conservative predictions of buckling loads. While current theories are accurate for most cylinders, few adequately account for the potential reduction in buckling load due to

transverse shear deformation when the cylinder has low radius-to-thickness (R/t) and length-to-radius (L/R) ratios.

A literature survey indicates that the problem of accounting for transverse-shear deformation effects has not been fully explored in the case of buckling of thick-walled laminated circular cylinders. A better understanding of transverse-shear deformation effects on the buckling of orthotropic and anisotropic thick-walled cylinders is needed to utilize fully laminated composites in aircraft applications.

1.2 Objectives and Scope

This report describes the results of an analytical study of the effects of transverse shear deformation and anisotropy on the buckling loads of circular cylinders subjected to either axial compression or a combination of axial compression and external pressure. Isotropic, symmetrically-laminated orthotropic and anisotropic circular cylinders are studied to determine which types of materials (e.g., isotropic metals, orthotropic and anisotropic graphite-epoxy composites), which stacking sequences (e.g., $[0]_{ns}$, $[90]_{ns}$, $[\pm 45/90]_{ns}$, $[45]_{ns}$), and which cylinder geometries (e.g., thin-walled long cylinders, thick-walled short cylinders) are most sensitive to transverse shear deformation. Mildly anisotropic and strongly anisotropic circular cylinders are studied to examine the effects of anisotropy on buckling loads.

1.3 Brief Review of Pertinent Literature

Several methods of accounting for transverse-shear deformation effects have been suggested in the literature for isotropic beams and plates. Timoshenko originally suggested the use of shear correction factors in reference 1. The use of shear correction factors for isotropic beams is not easily extended to account for changes in material properties through-the-thickness or to include the effects of curvature. Stavsky and Friedland assume non-constant material properties through-the-thickness in reference 2, but do not allow for a discontinuous distribution of the properties as is typical of laminated structures. Dong and Tso determine shear correction factors for orthotropic laminates in reference 3. In an attempt to avoid the use of shear correction factors, Levinson considers a plate theory with assumed cubic functions in the thickness direction in reference 4, but uses a variationally inconsistent set of equilibrium equations. This set of equations does not account for all of the strain energy correctly. The problem of accounting for transverse shearing in plates is studied in references 5 and 6 without the use of shear correction factors or inconsistent equations. Low stiffnesses in the thickness direction are common in laminated structures. The effect of low values for the Young's modulus and the shear modulus in the thickness direction for short, thick-walled cylinders is shown by Kaplan and Kan reference 7. Buckling loads are reduced substantially when these lower stiffnesses are taken into account.

Extensive work has been done in the area of buckling of thin-walled cylinders made of isotropic and orthotropic materials (e.g., refs. 8-12). The buckling of thin-walled cylinders usually involves little transverse

shear deformation. As the wall thickness increases, or the radius-to-thickness ratio decreases, the effects of transverse shear deformation on the buckling load become more pronounced. The importance of transverse shearing in composite shells is discussed in reference 13 where Vasil'ev compares the significance of a variety of effects which are neglected in classical Kirchoff-Love theory. Classical theory assumes that all normals to the reference surface of the undeformed structure must remain normal to the reference surface of the deformed structure. Vasil'ev concludes that for stability problems "allowance for radius variation through the thickness and for shear strain appears to be the most significant issues." This transverse-shearing-strain issue is addressed for sandwich cylinders in reference 14 where Stein and Mayers derive simple expressions to predict buckling loads of sandwich cylinders under axial compression. This analysis indicates that for a cylinder with a radius-to-thickness ratio of 10, the buckling load of a thick-walled sandwich cylinder is decreased by 50 percent or more compared to results from classical Kirchoff-Love theory. This decrease is due to transverse-shear deformation effects. Orthotropic and anisotropic cylinders can be studied by using the computer code which is described in reference 15. No conclusions are drawn about the effects of transverse shear deformation on buckling loads in reference 15.

One approach used to account for transverse-shear deformation effects more accurately is the use of more terms in the assumed displacement series than are used in classical Kirchoff-Love theory or in conventional Reissner-Mindlin first-order transverse-shear deformation theory. The inclusion of these additional terms results in a higher-order theory. In 1887 Levy included trigonometric terms in his assumed displacement series through-the-thickness for the displacements in the axial and circumferential directions

for the study of plates described in reference 16. In references 17 and 18 Stein develops a theory for studying buckling of cylinders based on nonlinear strain-displacement relations in which each assumed displacement series includes trigonometric terms in the through-the-thickness direction. These additional terms allow for more transverse shear deformation than in the classical or the first-order transverse-shear deformation theories. This higher-order theory can be used to calculate buckling loads of laminated shells.

The interaction between axial compressive loading and external pressure loading has been studied in reference 19 for thin-walled cylinders and in reference 20 for cylinders of moderate wall thicknesses. These studies do not address the potential problem of transverse shear deformation. Transverse-shear deformation effects can be important in predicting buckling loads of thick-walled cylinders subjected to external pressure loadings as well as to axial compressive loadings.

Laminate stacking sequence can have a significant effect on the buckling load of laminated cylinders. Several studies have been conducted to determine which stacking sequences are optimal and how many plies are needed for the assumption of constant material properties through-the-thickness to be valid (e.g., refs. 21-24). In reference 21, Onoda concludes that "one of the optimal configurations is shown to be the lamination with an infinite number of infinitely thin layers arranged so that the shell becomes quasi-isotropic in the shell surface and quasi-homogeneous through the thickness." However in reference 22, Uemura and Kasuya conclude that the effects of property changes from layer to layer decay rapidly as the number of layers is increased. The number of plies needed for constant material properties through the thickness to be assumed is dependent upon

the stacking sequence of the laminate. As few as six plies may be enough to assume constant material properties. Reference 23 includes a parametric study of stacking sequences in the family $[90,\theta]$ and concludes that the stacking sequences which lead to the highest buckling loads have $\theta = 45$ degrees while the stacking sequence which lead to the lowest buckling loads have $\theta = 90$ degrees. Reference 24 examines shells with $R/t = 50$ and $R/t = 150$ and finds that the optimal stacking sequence is unaffected by R/t in the cases studied. However, transverse-shear deformation effects are not adequately taken into account in the study on which reference 24 is based (reference 8). Anisotropic effects are studied in references 25 and 26 for plate buckling and in reference 27 for shell buckling but these studies do not include transverse-shear deformation effects. Anisotropic effects are discussed in references 28 and 29 for plates and curved panels, respectively.

The use of "correlation factors" or "knock-down" factors are recommended in reference 8 as a way of correlating experimental and analytical buckling loads. Reductions in buckling loads are suggested for isotropic sandwich cylinders subjected to axial compressive loadings to account for geometric imperfections which are not included in an analysis. These knock-down factors range from .3 (a 70 percent reduction in buckling load) for $R/t = 1000$ to .87 (a 13 percent reduction in buckling load) for $R/t = 10$. The sensitivity of axial compressive buckling loads to imperfections is not as significant for thick-walled cylinders as it is for thin-walled cylinders.

Most experimental studies of cylinder buckling due to axial compressive loadings concentrate on thin-walled cylinders and the effects of geometric imperfections. Most such studies involve thin-walled structures which would

not be expected to demonstrate significant transverse-shear deformation effects (e.g., refs. 30-31). One study which experimentally examines cylinders of moderate wall thicknesses is presented in reference 32. In that study the failure mode for applied axial compressive load is catastrophic shear failure for all cylinders of radius-to-thickness ratio less than 100. In reference 33, experimental results of buckling loads of cylinders subjected to axial compression with radius-to-thickness ratios as low as 100 are presented, but cylinder lengths are chosen to produce overall dimensions such that the cylinder would not be expected to demonstrate transverse-shear deformation effects. The analytical results in reference 33 include the region where transverse-shear deformation effects would appear if they were taken into account. No experimental results are presented for very short, thick-walled cylinders to support the theory.

The significance of transverse-shear deformation effects on the buckling load of a cylinder is dependent upon the cylinder geometry, the boundary conditions, the loading conditions, and, in the case of laminated cylinders, the stacking sequence and the degree of anisotropy. The effects of cylinder geometry, stacking sequence, and degree of anisotropy are addressed in this report. The method of analysis described in reference 17 is used to develop buckling equations for circular cylinders subjected to axial compressive and external pressure loadings. The effects of transverse shearing on the buckling loads of simply supported isotropic, orthotropic and anisotropic laminated circular cylinders is evaluated.

CHAPTER II

ANALYSIS APPROACH

The results presented in this report are obtained by applying the theory presented in reference 17. The buckling loads of circular cylinders are calculated by formulating and solving an eigenvalue problem. An assumed displacement series and the potential energy method are used to develop equilibrium equations. The equilibrium equations are converted to buckling equations and the buckling loads for cylinders subjected to axial compressive loadings or external pressure loadings are the eigenvalues of the problem. In formulating the problem, a consistent choice of linear and nonlinear terms in the strain-displacement relations is required. For the isotropic and orthotropic cylinders, the predicted buckling load is based on the assumption of one mode shape in the axial direction of the cylinder and one mode shape in the circumferencial direction. For the anisotropic cylinders, the predicted buckling load is based on the assumption of displacements in the form of a Fourier series in the axial direction.

2.1 Isotropic and Orthotropic Analysis

In reference 17 the potential energy method is used to obtain equations for the buckling of circular cylinders using a coordinate system with axes (x, θ, z), displacements (u, v, w), and cylinder dimensions (L, R, t) as shown in the sketch.

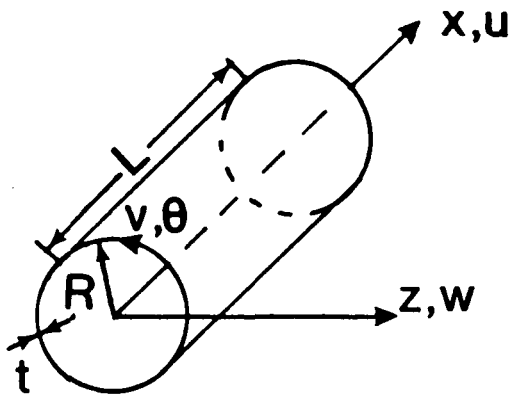

2.1.1 Formulation of Eigenvalue Problem

The dependence of the displacements on the z coordinate must be chosen to find the buckling load of a cylinder. Two series are assumed to represent the cylinder displacements which account for the higher-order effects of transverse shear deformation. The first assumed displacement series is given by equations (1).

$$
\begin{aligned}
u &= u^o + u^a\,(z/t) + u^1 \sin(\pi z/t) \\
v &= v^o + v^a\,(z/t) + v^1 \sin(\pi z/t) \\
w &= w^o + w^a\,(z/t) + w^1 \cos(\pi z/t)
\end{aligned}
\tag{1}
$$

The series in equations (1) have three types of terms, all of which are functions of x and θ. The traditional terms from classical Kirchhoff-Love theory (those independent of position in the radial direction) are represented by superscript o. Classical Kirchhoff-Love theory can be obtained by neglecting the superscript 1 terms and the w^a term and by assuming that $u^a = -w^o{}_{,x}$ and that $v^a = -w^o{}_{,y}$ in equations (1). The

additional terms associated with conventional Reissner-Mindlin first-order transverse-shear deformation theory (those linear in z) are represented by superscript a. Conventional Reissner-Mindlin first-order transverse-shear deformation theory can be obtained by neglecting the superscript 1 and the w^a terms. The assumed displacement series also includes trigonometric terms in the through-the-thickness (radial) direction, which are represented by the terms with superscript 1. Including additional terms (trigonometric in this case) in the assumed displacement series is expected to lead to more accurate solutions because more three-dimensional effects are permitted than in solutions with fewer assumed displacement terms. The second displacement series assumed to represent the higher-order through-the-thickness effects uses polynomial terms instead of trigonometric terms in z. In this case, a $(z/t)^3$ term is substituted for each $\sin(\pi z/t)$ and a $(z/t)^2$ term is substituted for each $\cos(\pi z/t)$ in equations (1).

Differential equations and boundary conditions for predicting the buckling loads of circular cylinders are developed in reference 17 by using the potential energy method and the assumed displacement series with the trigonometric terms in z given in equations (1). The virtual work found by using the potential energy method can be represented as shown in equation (2).

$$\delta \Pi = \int_{Vol} \{\sigma_x \delta\epsilon_x + \sigma_\theta \delta\epsilon_\theta + \sigma_z \delta\epsilon_z + \tau_{x\theta}\delta\gamma_{x\theta} + \tau_{xz}\delta\gamma_{xz} + \tau_{z\theta}\delta\gamma_{z\theta}\} \, d\,Vol \tag{2}$$

where σ_x, σ_θ, σ_z, $\tau_{x\theta}$, τ_{xz}, and $\tau_{\theta z}$ are the stresses and ϵ_x, ϵ_θ, ϵ_z, $\gamma_{x\theta}$, γ_{xz}, and $\gamma_{\theta z}$ are the strains in the cylinder. The transverse normal strain is included in the virtual work equation for completeness even though its contribution is expected to be small.

A linear prebuckling response is assumed and prebuckling boundary conditions are taken to be: displacements $v = w = 0$, normal force $\int_{-t/2}^{t/2} \sigma_x \, dz = N_x$, and moments $\int_{-t/2}^{t/2} \sigma_x \, (z/t) \, dz = 0$ and $\int_{-t/2}^{t/2} \sigma_x \, \sin(\pi z/t) \, dz = 0$ at $x = 0$ and $x = L$. The cylinder is assumed to expand uniformly in the lateral direction.

In reference 17 the strains in equations (2) are represented in terms of displacements of the form of equations (1). The resulting expression of the virtual work is broken up into one equation for each assumed displacement term, nine equations for nine unknowns, and are presented in equations (3).

$$\int_{-t/2}^{t/2} [\sigma_{x,x} + \frac{\tau_{x\theta,x}}{R} + (\frac{\sigma_\theta}{R^2} u^o_{,\theta})_{,\theta}] \delta u^o dz = 0$$

$$\int_{-t/2}^{t/2} [\frac{\sigma_{\theta,\theta}}{R} + \tau_{x\theta,x} + \frac{\tau_{\theta z}}{R} + (\sigma_x v^o_{,x})_{,x} + (\frac{\sigma_\theta}{R^2} w^o_{,\theta})_{,\theta} - \frac{\sigma_\theta}{R^2} v^o] \delta v^o dz = 0$$

$$\int_{-t/2}^{t/2} [- \frac{\sigma_\theta}{R} + \tau_{xz,x} + \frac{\tau_{\theta z,\theta}}{R} + (\sigma_x w^o_{,x})_{,x} + (\frac{\sigma_\theta}{R^2} w^o_{,\theta})_{,\theta} - (\frac{\sigma_\theta}{R^2} v^o)_{,\theta}] \delta w^o dz = 0$$

$$\int_{-t/2}^{t/2} [(\sigma_{x'x} + \frac{\tau_{x\theta'\theta}}{R}) \frac{z}{t} - \frac{\tau_{xz}}{t}] \delta u^a dz = 0$$

$$\int_{-t/2}^{t/2} [(\frac{\sigma_{\theta'\theta}}{R} + \tau_{x\theta'x}) \frac{z}{t} - \frac{\tau_{\theta z}}{t} + \frac{\tau_{\theta z}}{R} \frac{z}{t}] \delta v^a dz = 0 \qquad (3)$$

$$\int_{-t/2}^{t/2} [(- \frac{\sigma_\theta}{R} + \tau_{xz'x} + \frac{\tau_{\theta z'\theta}}{R}) \frac{z}{t} + \frac{\sigma_z}{t}] \delta w^a dz = 0$$

$$\int_{-t/2}^{t/2} [(\sigma_{x'x} + \frac{\tau_{x\theta'\theta}}{R}) \sin (\frac{\pi z}{t}) - \tau_{xz} \frac{\pi}{t} \cos (\frac{\pi z}{t})] \delta u^1 dz = 0$$

$$\int_{-t/2}^{t/2} [(\frac{\sigma_{\theta'\theta}}{R} + \tau_{x\theta'x}) \sin (\frac{\pi z}{t}) - \frac{\pi}{t} \tau_{\theta z} \cos (\frac{\pi z}{t}) + \frac{\tau_{\theta z}}{R} \sin (\frac{\pi z}{t})] \delta v^1 dz = 0$$

$$\int_{-t/2}^{t/2} [(- \frac{\sigma_\theta}{R} + \tau_{xz'x} + \frac{\tau_{\theta z'\theta}}{R}) \cos (\frac{\pi z}{t}) + \frac{\pi}{t} \sigma_z \sin (\frac{\pi z}{t})] \delta w^1 dz = 0$$

where δu^o, δu^a, δu^1, ... are the displacement variations. The equilibrium equations for the cylinder are obtained from equations (3) by integrating by parts.

The differential equations of equilibrium can be converted to buckling equations by considering small changes in deformations that occur at buckling. This assumption reduces the first, second and third equations of equations (3) to:

$$\int_{-t/2}^{t/2} [\sigma_{x',x} + \frac{\tau_{x\theta',\theta}}{R}] \, \delta u^o dz = 0$$

$$\int_{-t/2}^{t/2} [\frac{\sigma_{\theta',\theta}}{R} + \tau_{x\theta',x} + \frac{\tau_{\theta z}}{R}] \, \delta v^o dz = 0 \tag{4}$$

$$\int_{-t/2}^{t/2} [- \frac{\sigma_\theta}{R} + \tau_{xz',x} + \frac{\tau_{\theta z',\theta}}{R}] \, \delta w^o dz = 0$$

while the other equations of equations (3) remain unchanged.

The differential equations represented by equations (3) and (4) can be reduced to linear equations containing only the displacement and loading terms as unknowns by using the following stress-strain and strain-displacement relations as derived in references 17 and 34.

$$\{\sigma\} = [C_{ij}] \{\epsilon\}$$

$$\epsilon_x = u,_x + \frac{1}{2} (w,_x^2 + v,_x^2)$$

$$\epsilon_\theta = \frac{1}{2R^2} (u,_\theta^2 + (w,_\theta - v)^2) + \frac{1}{R}(w + v,_\theta)$$

$$\epsilon_z = \frac{w^a}{t} - w^1 \frac{\pi}{t} \sin (\frac{\pi z}{t}) \tag{5}$$

$$\gamma_{x\theta} = \frac{u,_\theta}{R} + v,_x + \frac{w,_x}{R} (w,_\theta - v) - \frac{u,_\theta}{R} (v,_\theta + w) - v,_x u,_x$$

$$\gamma_{xz} = \frac{u^a}{t} + \frac{\pi}{t} u^1 \cos\left(\frac{\pi z}{t}\right) + w_{,x} - u_{,x} w_{,x}$$

$$\gamma_{\theta z} = \frac{v^a}{t} + \frac{\pi}{t} v^1 \cos\left(\frac{\pi z}{t}\right) + \frac{1}{R}(w_{,\theta} - v) - \frac{1}{R^2}(w + v_{,\theta})(w_{,\theta} - v)$$

where $[C_{ij}]$ is the orthotropic material stiffness matrix. For orthotropic laminates, the number of plies in the laminate is assumed to be large enough that the cylinder can be assumed to be transversely isotropic.

The dependence of the displacements on the axial and circumferencial coordinates can be expressed in the form:

$$\begin{aligned} u &= [U^o + U^a (z/t) + U^1 \sin(\pi z/t)] \cos(m\pi x/L) \sin(n\theta) \\ v &= [V^o + V^a (z/t) + V^1 \sin(\pi z/t)] \sin(m\pi x/L) \cos(n\theta) \\ w &= [W^o + W^a (z/t) + W^1 \cos(\pi z/t)] \sin(m\pi x/L) \sin(n\theta) \end{aligned} \tag{6}$$

where the superscripted terms are constants (independent of position). The cylinder buckle pattern is assumed to consist of m half waves in the longitudinal direction and n full waves in the circumferential direction.

The displacements used to find the critical buckling load (bifurcation buckling point) are shown in equations (7).

$$\begin{aligned} \tilde{u} &= u + \bar{u} \\ \tilde{v} &= v + \bar{v} \\ \tilde{w} &= w + \bar{w} \end{aligned} \tag{7}$$

The displacements $\tilde{u}$, $\tilde{v}$, and $\tilde{w}$, contain u, v, and w, as defined in equations (6) . The displacements $\bar{u}$, $\bar{v}$, and $\bar{w}$ are assumed to be the small changes in displacements which occur at buckling. These small displacements are assumed to be in the same form as the prebuckling displacements in their dependence on x, θ, and z (e.g. $\bar{u}$ contains components $\bar{u}^o$, $\bar{u}^a$, and $\bar{u}^1$). Simple support buckling boundary conditions $w = w,_{xx} = v = u,_x = 0$ are assumed.

Substituting equations (5) and (6) into equations (3) and (4) and integrating in the radial direction gives the following linear equations:

$$\alpha\bar{u}^o + \beta\bar{v}^o + \psi\bar{w}^o + \frac{2}{\pi}\psi\,\bar{w}^1 = 0$$

$$\beta\bar{u}^o + \Delta\bar{v}^o + \kappa\bar{w}^o - \xi\bar{v}^a + 2\xi\bar{v}^1 + \frac{2}{\pi}\kappa\,\bar{w}^1 = 0$$

$$\psi\bar{u}^o + \kappa\bar{v}^o + \eta\bar{w}^o + G_{xz}\frac{m\pi}{L}\bar{u}^a + \xi n\bar{v}^a + G_{xz}\frac{2m\pi}{L}\bar{u}^1 + 2n\xi\bar{v}^1 + \frac{2}{\pi}\eta\,\bar{w}^1 = 0$$

$$G_{xz}\frac{m\pi}{L}\bar{w}^o + \left(\frac{\alpha}{12} + \frac{G_{xz}}{t}\right)\bar{u}^a + \frac{\beta}{12}\bar{v}^a + \frac{\psi}{12}\bar{w}^a + \left(\frac{\alpha}{\pi^2} + G_{xz}\frac{2}{t}\right)\bar{u}^1 + \frac{\beta}{\pi^2}\bar{v}^1 + G_{xz}\frac{2m}{L}\bar{w}^1 = 0$$

$$-\xi\bar{v}^o + \xi n\bar{w}^o + \frac{\beta}{12}\bar{u}^a + [\Delta/12 + G_{z\theta}/t]\bar{v}^a + \frac{\kappa}{12}\bar{w}^a + \beta\bar{u}^1 + [\Delta/\pi^2 + \frac{2}{t}G_{z\theta}]\,\bar{v}^1 + \xi\frac{2n}{\pi}\bar{w}^1 = 0$$

$$\psi/12\ \bar{u}^a + \frac{\kappa}{12}\ \bar{v}^a + \left(\frac{\eta}{12} + \frac{Q_{33}}{t}\right)\ \bar{w}^a + \frac{\psi}{\pi^2}\ \bar{u}^1 + \frac{\kappa}{\pi^2}\ \bar{v}^1 = 0 \tag{8}$$

$$G_{xz}\frac{2m\pi}{L}\ \bar{w}^o + \left(\frac{\alpha}{\pi^2} + G_{xz}\left(\frac{2\pi}{t}\right)\right)\ \bar{u}^a + \beta/\pi^2\ \bar{v}^a + \frac{\psi}{\pi^2}\ \bar{w}^a + \frac{1}{2}\left(\alpha + G_{xz}\frac{\pi^2}{t}\right)\ \bar{u}^1$$

$$+ \frac{1}{2}\beta\ \bar{v}^1 + G_{xz}\frac{m\pi^2}{2L}\ \bar{w}^o = 0$$

$$-\xi\ \frac{2}{\pi}\ \bar{v}^o + \xi 2n\ \bar{w}^o + \beta/\pi^2\ \bar{u}^a + \left[\Delta/\pi^2 + \frac{2}{t}\ G_{z\theta}\right]\ \bar{v}^a + \frac{\kappa}{\pi^2}\ \bar{w}^a + \frac{\beta}{2}\ \bar{u}^1 +$$

$$\left[\Delta + \frac{\pi^2}{t}\ G_{z\theta}\right]\ \frac{\bar{v}^1}{2} + \frac{n\pi}{2}\xi\ \bar{w}^1 = 0$$

$$\frac{2}{\pi}\xi\ \bar{u}^o + \frac{2}{\pi}\kappa\ \bar{v}^o + \frac{2}{\pi}\ \eta\ \bar{w}^o + G_{xz}\frac{2m}{L}\ \bar{u}^a + \xi\frac{2n}{\pi}\ \bar{v}^a + G_{xz}\frac{m\pi^2}{2L}\ \bar{u}^1 + \frac{n\pi}{2}\ \xi\ \bar{v}^1 +$$

$$\left(\eta + \frac{\pi^2}{t}\ C_{33}\right)\ \frac{1}{2}\ \bar{w}^1 = 0$$

where $\alpha = [C_{11}(m\pi/L)^2 + G_{x\theta}(n/R)^2]\ t$

$\beta = (C_{12} + G_{x\theta})\ m\ n\ \pi\ t\ /(R\ L)$

$\psi = -C_{12}\ m\ t\ \pi\ /(R\ L)$

$\Delta = [C_{22}\ (n/R)^2 + G_{x\theta}(m\pi/L)^2 + G_{z\theta}/R^2]\ t$

$\kappa = -(C_{22} + G_{x\theta})(n/R)^2\ t$

$\eta = [C_{22}/R^2 + G_{xz}(m\pi/L)^2 + G_{z\theta}\ (n/R)^2]\ t$

$\xi = G_{z\theta}/R$

and C_{11}, C_{12}, C_{22}, $G_{x\theta}$, G_{xz}, and $G_{\theta x}$ are properties of the cylinder wall. For metallic isotropic cylinders, equations (7) are simplified such that $C_{11} = C_{22} = C_{33} = E/(1-\mu^2)$, $C_{12} = \mu C_{11}$, and $G_{xz} = G_{x\theta} = G_{\theta z} = G = E/2(1+\mu)$ where E is Young's modulus and μ is Poisson's ratio.

Loading terms for uniform axial compression and uniform external pressure are added to the first, second and third of equations (8) where N_x and P are the constants which represent the magnitude of the axial load and the external pressure, respectively, in equations (9).

$$N_x = \int \sigma_x \, dz \tag{9}$$

$$P\,R = \int \sigma_\theta \, dz = N_\theta$$

Buckling loads can be found by reducing equations (8) (with the loading terms added to the right hand side) to matrix form as shown in equation (10).

$$[K] \begin{Bmatrix} \bar{u}^o \\ \bar{v}^o \\ \bar{w}^o \\ \bar{u}^a \\ \bar{v}^a \\ \bar{w}^a \\ \bar{u}^1 \\ \bar{v}^1 \\ \bar{w}^1 \end{Bmatrix} - \left(N_x \, [B_1] + N_\theta \, [B_2] \right) \begin{Bmatrix} \bar{u}^o \\ \bar{v}^o \\ \bar{w}^o \\ \bar{u}^a \\ \bar{v}^a \\ \bar{w}^a \\ \bar{u}^1 \\ \bar{v}^1 \\ \bar{w}^1 \end{Bmatrix} \tag{10}$$

The matrix $[K]$ contains the coefficients of the linear displacement terms shown in equations (8). The matricies $[B_1]$ and $[B_2]$ contain the coefficients of the nonlinear displacement terms in equations (5) when substituted into equations (3) and (4).

The lowest value of N_x or N_θ which is a solution to the eigenvalue problem in equation (10) is the critical buckling load. The values of m and n which give the lowest N_x or N_θ represent the number of waves at buckling. If the buckling load of a cylinder subjected to a combination of loads is to be found, a value for N_x is chosen and substituted into equation (10) and the product of $N_x \, [B_1]$ times the displacement vector is moved to the left hand side of the equation. The eigenvalue problem can then be solved for N_θ.

A computer code was written to find buckling loads represented by N_x and N_θ in equation (10) for orthotropic (or mildly anisotropic) cylinders subjected to axial compressive or external pressure loadings. The eigenvalue is calculated using a library subroutine called CSQZ which is described in reference 35. This subroutine uses the combination shift QZ algorithm. A flow chart of the computer code used to find buckling loads of orthotropic cylinders subjected to axial compressive loadings is presented in figure 1.

2.1.2 Importance of Compatibility and Consistency in Strains

Several assumptions might be made for the nonlinear terms in the axial strain to obtain buckling equations for cylinders loaded in axial compression. Three possible assumptions are shown in equations (11).

$$
\begin{aligned}
\epsilon_x &= u,_x + \frac{1}{2}(w,_x)^2 + \frac{1}{2}(v,_x)^2 \\
\epsilon_x &= u,_x + \frac{1}{2}(w,_x)^2 \\
\epsilon_x &= u,_x + \frac{1}{2}(w^o,_x)^2
\end{aligned}
\tag{11}
$$

The first assumption includes all nonlinear components of the displacements v and w. An expanded form of the axial strain is found by substituting equations (1) into the first equation in equations (11), as shown in equation (12).

$$\epsilon_x = u,_x + \frac{1}{2}\left(w^o,_x + w^a,_x(z/t) + w^1,_x \cos(\pi z/t)\right)^2 + \frac{1}{2}\left(v^o,_x + v^a,_x(z/t) + v^1,_x \sin(\pi z/t)\right)^2 \tag{12}$$

When the nonlinear terms are squared as indicated, equation (12) includes 18 nonlinear terms. After integrating in the thickness direction, all 18 terms may be non-zero for an unsymmetric laminate. For a symmetric laminate, only 10 terms are non-zero as shown in the $[B_1]$ matrix in equation (13).

$$[B_1] = \begin{bmatrix} 0 & 0 & 0 & 0 & 0 & 0 & 0 & 0 & 0 \\ 0 & a & 0 & 0 & 0 & 0 & 0 & 0 & 0 \\ 0 & 0 & b & 0 & 0 & 0 & 0 & 0 & g \\ 0 & 0 & 0 & 0 & 0 & 0 & 0 & 0 & 0 \\ 0 & 0 & 0 & 0 & c & 0 & 0 & k & 0 \\ 0 & 0 & 0 & 0 & 0 & d & 0 & 0 & 0 \\ 0 & 0 & 0 & 0 & 0 & 0 & 0 & 0 & 0 \\ 0 & 0 & 0 & 0 & k & 0 & 0 & e & 0 \\ 0 & 0 & g & 0 & 0 & 0 & 0 & 0 & f \end{bmatrix} (m\pi/L)\ t \tag{13}$$

In equation (13), $a=b=1$, $c=d=1/12$, $e=f=1/2$, $g=2/\pi$, and $k=2/\pi^2$ for the assumed trigonometric displacements in equations (1), and $a=b=1$, $c=d=1/12$, $e=1/448$, $g=1/12$, $f=1/80$, and $k=1/16$ for the assumed polynomial displacements in the thickness direction.

Use of the second assumption in equations (11) requires that $a=c=e=k=0$ in equation (13). This simplification neglects all the nonlinear v displacements by assuming that their contribution is small compared to the

contribution of the w displacements. Use of the third assumption in equations (11) requires that all terms in $[B_1]$ in equation (13) are equal to zero except b=1. This simplification neglects all nonlinear v and w displacement terms except the constant term through the thickness in w, which is w^o.

The third assumption of equations (11) can be justified if the v displacements are negligible compared to the w displacements and the w^a and w^1 terms are negligible compared to w^o. The third assumption may seem to be a logical choice since it is the simplest and all neglected terms are expected to be small relative to w^o.

The assumptions used for the strains and displacements must satisfy the compatibility conditions for three-dimensional shells. Three-dimensional compatibility equations are presented in reference 36 as "conditions of compatibility" and are given, using the previously defined coordinates, in equations (14).

$$\frac{1}{\bar{R}^2}\epsilon_{x'\theta\theta} + \epsilon_{\theta'xx} = \frac{1}{\bar{R}}\gamma_{x\theta'x\theta}$$

$$\frac{2}{\bar{R}}\epsilon_{x'\theta z} = -\frac{1}{\bar{R}}\gamma_{\theta z'xx} + \frac{1}{\bar{R}}\gamma_{xz'\theta x} + \gamma_{x\theta'xz}$$

$$2\,\epsilon_{\theta'xz} = \frac{1}{\bar{R}}\gamma_{\theta z'x\theta} - \frac{1}{\bar{R}^2}\gamma_{xz'\theta\theta} + \frac{1}{\bar{R}}\gamma_{x\theta'z\theta} \tag{14}$$

$$\frac{2}{\bar{R}}\epsilon_{z,x\theta} = \gamma_{\theta z'xz} + \frac{1}{\bar{R}}\gamma_{xz'\theta z} - \gamma_{x\theta'zz}$$

$$\epsilon_{\theta' zz} + \frac{1}{R^2}\,\epsilon_{z'\theta\theta} = \frac{1}{R}\,\gamma_{\theta z'\theta z}$$

$$\epsilon_{z'xx} + \epsilon_{x'zz} = \gamma_{xz'xz}$$

The linear parts of the strains and displacements must satisfy the compatibility conditions. The sine and cosine waves in the displacements in the x and θ directions in equations (6) are chosen to satisfy the compatibility conditions of reference 36. If the linear components of equations (5) and (6) are substituted into equations (14), and the differentiation with respect to x and θ is performed, the dependence of equations (14) upon x and θ is removed and all prebuckling conditions are satisfied.

The nonlinear strains must also satisfy the compatibility conditions. The only strain which contains nonlinear terms is the axial strain. The last three conditions in equations (14) are independent of the axial strain so the assumption used for the axial strain will not affect them. When the strains defined in equations (5), including the first assumption in equations (11) for the axial strain, are substituted into the first three equations of (14), these three compatibility conditions become:

$$\frac{1}{\bar{R}^2} u_{,x\theta\theta} + \frac{1}{2}\frac{1}{\bar{R}^2} (w_{,x}^{\ 2})_{,\theta\theta} + \frac{1}{2}\frac{1}{\bar{R}^2} (v_{,x}^{\ 2})_{,\theta\theta} + \frac{1}{\bar{R}} v_{,xx\theta} + \frac{1}{\bar{R}} w_{,xx}$$

$$= \frac{1}{\bar{R}^2} u_{,x\theta\theta} + \frac{1}{\bar{R}} v_{,xx\theta}$$

$$\frac{2}{\bar{R}} u_{,xz\theta} + \frac{2}{\bar{R}} \{\frac{1}{2}\frac{1}{\bar{R}} (w_{,x}^{\ 2})_{,z\theta} + \frac{1}{2}\frac{1}{\bar{R}} (v_{,x}^{\ 2})_{,z\theta}\} = \tag{15}$$

$$- \frac{1}{\bar{R}} (v_{,z} + \frac{1}{\bar{R}} w_{,\theta} - \frac{1}{\bar{R}} v)_{,xx} + \frac{1}{\bar{R}} (u_{,z} + w_{,x})_{,x\theta} + (\frac{1}{\bar{R}} u_{,\theta} + v_{,x})_{,xz}$$

$$u_{,xzz} + \frac{1}{2} (w_{,x}^{\ 2})_{,zz} + \frac{1}{2} (v_{,x}^{\ 2})_{,zz} + w_{,zxx} = u_{,zxz} + w_{,xxz}$$

These three conditions are satisfied since the same displacement assumptions are made in each term in each equation. The first assumed axial strain of equations (11) is valid.

If the second assumption of equations (11) is used, the first three conditions in equations (14) are also satisfied. The compatibility is shown in equation (16) for the first compatibility condition by substituting the second assumption of equations (11) for the axial strain into the first equation of (14).

$$\frac{1}{\bar{R}^2} u_{,x\theta\theta} + \frac{1}{2}\frac{1}{\bar{R}^2} (w_{,x}^{\ 2})_{,\theta\theta} + \frac{1}{\bar{R}} v_{,xx\theta} + w_{,xx} = \frac{1}{\bar{R}^2} u_{,x\theta\theta} + \frac{1}{\bar{R}} v_{,xx\theta} \tag{16}$$

However, when the third assumption for axial strain in equations (11) is substituted into the first three compatibility conditions of equations ( ), equations (17) result.

$$\frac{1}{R^2} u_{,x\theta\theta} + \underline{\frac{1}{2}\frac{1}{R^2}(w^o{}_{,x}{}^2)_{,\theta\theta}} + \frac{1}{R} v_{,xx\theta} + \underline{w_{,xx}} = \frac{1}{R^2} u_{,x\theta\theta} + \frac{1}{R} v_{,xx\theta}$$

$$\frac{2}{R} u_{,xz\theta} + \underline{\frac{1}{2}\frac{1}{R}(w^o{}_{,x}{}^2)_{,z\theta}} = -\frac{1}{R}(v_{,z} + \underline{\frac{1}{R} w_{,\theta}} - \frac{1}{R} v)_{,xx} \tag{17}$$

$$+ \frac{1}{R}(u_{,z} + \underline{w_{,x}})_{,x\theta} + (\frac{1}{R} u_{,\theta} + v_{,x})_{,xz}$$

$$u_{,xzz} + \underline{\frac{1}{2}(w^o{}_{,x}{}^2)_{,zz}} + \underline{w_{,zxx}} = u_{,zxz} + v_{,xxz}$$

Since w without a superscript includes w^o, w^a, and w^1, the linear terms in w in equations (17) include the w^a and w^1 terms. The nonlinear terms do not contain the w^a and w^1 terms. Linear and nonlinear out-of-plane displacement terms are included in all three equations of (17), as shown by the underlined terms. These equations are based on two different assumptions for w in the same equation. These three compatibility conditions do not make consistent assumptions about the out-of-plane displacement. Therefore, the last assumption in equations (11), namely, neglecting the nonlinear w^a and w^1 terms in the axial strain but including them in the linear components, is not a valid assumption. Buckling loads calculated from equations with the valid assumptions and the invalid assumption are compared in the results section.

2.2 Anisotropic Analysis

The formulation of the eigenvalue problem for anisotropic cylinders is similar to the formulation of the eigenvalue problem for orthotropic

cylinders. The same equilibrium and strain-displacement equations are used in the analysis of the anisotropic cylinders as in the analysis of the orthotropic cylinders, as shown in equations (2-5). The stress-strain equations are altered to include the anisotropic effects which are represented by the C_{16} and C_{26} terms in equations (18).

$$\begin{aligned} \sigma_x &= C_{11}\,\epsilon_x + C_{12}\,\epsilon_\theta + C_{16}\gamma_{x\theta} \\ \sigma_\theta &= C_{12}\,\epsilon_x + C_{22}\,\epsilon_\theta + C_{26}\gamma_{x\theta} \\ \tau_{x\theta} &= C_{16}\,\epsilon_x + C_{26}\,\epsilon_\theta + C_{66}\gamma_{x\theta} \end{aligned} \tag{18}$$

Transverse isotropy is not assumed for the anisotropic solution so each integral in the radial direction must be evaluated for each ply. For some laminates this method of evaluation provides a more accurate buckling load than assuming transverse isotropy (ref. 22). The displacements used in the anisotropic analysis are similar to those given in equations (6), but the series are expanded to include the sum of several values of m while retaining only one value of n. Several values of m are included to account for displacements in the axial direction which are not in the shape of a pure sine wave. Two Fourier series in the axial direction are used to represent the displacements in the radial direction. One series includes symmetric modes and one series includes antisymmetric modes. Each series is truncated when enough terms have been included to reach convergence. Similar assumptions are made for the displacement series in the axial and circumferencial directions. The assumed displacements for an anisotropic cylinder are given in equations (19) where a total of N terms are included in each displacement.

$$u = \sum_{i=1,3,5}^{N} [U_i^o + U_i^a (z/t) + U_i^1 \sin(\pi z/t)] \cos(m_i \pi x/L) \sin(n\theta)$$

$$+ \sum_{j=2,4,6}^{N} [U_j^o + U_j^a (z/t) + U_j^1 \sin(\pi z/t)] \cos(m_j \pi x/L) \cos(n\theta)$$

$$v = \sum_{i=1,3,5}^{N} [V_i^o + V_i^a (z/t) + V_i^1 \sin(\pi z/t)] \sin(m_i \pi x/L) \cos(n\theta)$$

$$+ \sum_{j=2,4,6}^{N} [V_j^o + V_j^a (z/t) + V_j^1 \sin(\pi z/t)] \sin(m_j \pi x/L) \sin(n\theta) \quad (19)$$

$$w = \sum_{i=1,3,5}^{N} [W_i^o + W_i^a (z/t) + W_i^1 \sin(\pi z/t)] \sin(m_i \pi x/L) \sin(n\theta)$$

$$+ \sum_{j=2,4,6}^{N} [W_j^o + W_j^a (z/t) + W_j^1 \sin(\pi z/t)] \sin(m_j \pi x/L) \cos(n\theta)$$

The same procedure for reducing the differential equations of equilibrium to linear equations used for the analysis of the orthotropic cylinders is used for the analysis of the anisotropic cylinders. The same boundary and prebuckling conditions assumed for the orthotropic analysis are assumed for the anisotropic analysis. There are nine equations and nine unknown displacements for each value of m for the displacements represented by equations (19). The matrix $[K]_{ANISO}$ contains all the orthotropic terms in $[K]$ for several axial wavelengths (mode shapes) and the anisotropic terms which result from the combination of wavelengths. Similarly, the geometric stiffness matricies of the anisotropic cylinder, $[B_1]_A$ and $[B_2]_A$, contain all the terms found in $[B_1]$ and $[B_2]$, respectively, for several mode shapes instead of only one. Therefore, for 5

values of m, N=5 in equations (19), and the matricies $[K]_{ANISO}$, $[B_1]_A$, and $[B_2]_A$ have dimensions 45 by 45. The eigenvalue problem whose solution is the buckling load of an anisotropic cylinder subjected to axial compression or external pressure loadings is shown in equation (20).

$$[K]_{ANISO}\begin{Bmatrix} \bar{u}_1^o \\ \bar{v}_1^o \\ \bar{w}_1^o \\ \bar{u}_1^a \\ \cdot \\ \cdot \\ \cdot \\ \bar{w}_N^a \\ \bar{u}_N^1 \\ \bar{v}_N^1 \\ \bar{w}_N^1 \end{Bmatrix} = \left(N_x\ [B_1]_A + N_\theta\ [B_2]_A\right)\begin{Bmatrix} \bar{u}_1^o \\ \bar{v}_1^o \\ \bar{w}_1^o \\ \bar{u}_1^a \\ \cdot \\ \cdot \\ \cdot \\ \bar{w}_N^a \\ \bar{u}_N^1 \\ \bar{v}_N^1 \\ \bar{w}_N^1 \end{Bmatrix} \tag{20}$$

The number of mode shapes which needs to be included in equations (20) to obtain an accurate buckling load is dependent on the geometry and properties of the cylinder. Including an infinite number of mode shapes would give the most accurate solution. Approximate solutions are obtained by using a limited number of mode shapes. The more mode shapes used, the

more accurate is the buckling load, but as each additional mode shape is added, the difference between buckling loads predicted by equation (20) with N and with $N+1$ mode shapes decreases until the predicted load has converged to the same buckling load as predicted by an infinite number of mode shapes. The buckling load is the minimum value of N_x or N_θ which is a solution to equation (20) and n is the number of waves around the circumference. The eigenvalue is found by using the same subroutine for the anisotropic cylinder as for the orthotropic cylinder. The buckling load due to a combination of loads is found by assuming a value for N_x, moving the product of $N_x\,[B_1]_A$ times the vector of displacements to the left hand side of the equation and solving for N_θ.

Since many mode shapes may be needed to obtain an accurate buckling load and buckle pattern, solving the full system of equations may not be the most cost-effective approach in terms of computer requirements. A reduction method is presented in reference 25 by which the size of the matricies $[K]_{ANISO}$, $[B_1]_A$, the displacement vector and the size of the system of equations to be solved can be reduced. This reduced eigenvalue problem can be used to find the buckling load of the anisotropic cylinder.

2.3 Shear Correction Factors

An alternate method of accounting for transverse-shear deformation effects in calculating global structural responses, such as buckling loads, is the use of shear correction factors. Shear correction factors are used in references 3, 37, and 38 to calculate buckling loads in laminated plates

and shells. Buckling loads based on these shear correction factors are compared to results of the previously described orthotropic analysis in the results section.

2.4 Sensitivity to Anisotropy

A parameter for evaluating how significant anisotropic effects are on the buckling load of laminated panels is developed in reference 25. A similar parameter can be determined for cylinders by using the matricies in equation (20) without solving the eigenvalue problem of the anisotropic cylinder. The development of this parameter is outlined in Appendix A and a comparison of its values for various cylinders is presented in the results section.

CHAPTER III

RESULTS AND DISCUSSION

Buckling loads for isotropic and laminated cylinders subjected to axial compressive and/or external pressure loadings are determined from the higher-order transverse-shear deformation theory and compared to buckling loads predicted by classical and first-order transverse-shear deformation theories. The cylinders are assumed to be simply supported and without any initial geometric imperfections.

3.1 Axial Compression

The addition of either trigonometric or polynomial terms in the thickness direction to the constant and linear terms of first-order transverse-shear deformation theory reduces cylinder buckling loads equally. For all the geometries of isotropic and laminated composite cylinders studied, the present higher-order theory based on trigonometric terms in the assumed displacements predicted a buckling load within one percent of the buckling load predicted by the present higher-order theory based on polynomial terms in the assumed displacements. Adding more than one term to the displacement series (such as $\sin(3\pi z/t)$ or $(z/t)^5$ as well as $\sin(\pi z/t)$ or $(z/t)^3$) does not decrease the predicted buckling load by more than 2 percent for isotropic or laminated cylinders of a variety of geometries. Only one term in each displacement direction needs to be added to the displacement series of first-order transverse-shear deformation theory for the eigenvalues to converge for either trigonometric or polynomial assumed

displacement terms. Since the same buckling load results from assuming either polynomial or trigonometric terms in the assumed displacements, the term "present theory" in the following text and figures refers to the higher-order theory described in the previous chapter using either trigonometric or polynomial terms in the assumed displacements.

3.1.1 Consistency and Compatibility Requirements

Buckling loads resulting from each for the three assumptions of axial strain presented in equations (11) and classical and first-order transverse-shear deformation theories are presented in figure 2. The buckling load and cylinder dimensions are expressed in terms of nondimensional parameters Z, k_x and t/L, which are a curvature parameter, a compressive load coefficient, and a geometric cylinder parameter, respectively. These parameters are discussed in more detail in the next section. The actual values of these parameters and the specific material properties are not important in comparing the effects of different assumptions for axial strain since the curves shown are typical of the isotropic and laminated cylinders studied. The three assumptions for axial strain in equations (11) are: 1) all nonlinear v and w terms are included; 2) all nonlinear v terms are neglected; and 3) all nonlinear v and nonconstant w terms are neglected.

The first and second assumptions of axial strain are valid but the third is not, as discussed in the previous chapter. Two points can be made by comparing the buckling loads predicted by the present theory based on the three assumptions. First, when the nonlinear terms in v are neglected,

the same buckling load is predicted as when they are included, so the nonlinear terms in v apparently can be neglected. The first and second assumptions in equations (11) are valid and predict the same buckling loads, represented by the curve with short dashes in figure 2. Secondly, when some of the nonlinear w terms are neglected, as in the third assumption of equations (11) (the invalid assumption), the resulting buckling load is significantly lower than when the valid assumptions are made, represented by the curve with long dashes in the figure. The three solutions agree with the classical and first-order transverse-shear deformation theories for long, thin cylinders with low values of Z. However, for cylinders with high values of Z, the invalid assumption (neglecting the out-of-plane displacement terms, w^a and w^1, in the nonlinear parts of the strains but including them in the linear parts of the strains) leads to buckling loads which are as much as 80 percent lower than the buckling loads predicted using a valid assumption in the strains. Assumptions which satisfy the compatibility conditions must be used to obtain accurate buckling loads. Invalid assumptions can lead to incorrect and misleading results.

3.1.2 Buckling of Orthotropic and Mildly Anisotropic Cylinders

3.1.2.1 Isotropic Cylinders

Isotropic cylinders with a wide range of geometries and the properties of aluminum ($E=10.5 \times 10^6$ psi and $\mu = 1/3$) are studied to determine the effects of transverse shear deformation on axial compressive buckling loads. The buckling loads predicted by three theories are shown in figure 3 in

terms of nondimensional parameters $k_x = N_x L^2/(D \pi^2)$, $s = D \pi^2/(G t L^2)$, and $Z = L^2\sqrt{(12 (1 - \mu^2))}/(R t)$ where D is the bending stiffness and G is the shear stiffness of the shell wall. The nondimensional parameter Z is a useful parameter which represents the curvature of isotropic cylinders. However, numerical values of Z do not provide an intuitive "feel" for the geometry of the cylinder. Reference 9 includes a comparison of several cylinder geometries which have the same values of Z and explains its physical significance for low values. For isotropic cylinders, Z is directly proportional to $L^2/(Rt)$, which can also be expressed as $(R/t)(L/R)^2$. Cylinders with different radius-to-thickness ratios can have the same value of Z if the lengths are adjusted. Three cylinders which have the same value of Z are cylinders with: 1) $R/t=1.4$, $L/R=14$; 2) $R/t=11$, $L/R=5$; and 3) $R/t=68$, $L/R=2$. The first of these cylinders has an extremely thick wall and is fairly long while the second is short but with a slightly thinner wall. The third cylinder is of moderate thickness but is very short.

The three theories used to predict the buckling loads shown in figure 3 are: 1) the classical theory without transverse shear deformation; 2) the first-order transverse-shear deformation theory of reference 14; and 3) the present higher-order shear deformation theory using assumed trigonometric or polynomial displacements in the thickness direction. Results for four geometric configurations, indicated by different values of s, are shown in the figure. All theories give essentially the same buckling load for thin-walled cylinders (small values of Z). When no transverse shear deformation is assumed, k_x increases as Z increases for all values

of Z (classical theory). However, results from buckling loads based on the theory of reference 14, in which transverse shear deformation is included, indicate that transverse shear deformation is important even in isotropic cylinders and can reduce the buckling load by 50 percent or more for thick-walled cylinders. This reduction is indicated by k_x becoming constant in figure 3 as Z increases above a certain value of Z that depends on s. The dashed lines in figure 3 represent the buckling loads obtained from the present theory using through-the-thickness trigonometric or polynomial terms. For all values of s considered, the present higher-order theory decreases the predicted buckling load by no more than a few percent compared to the buckling load predicted by the first-order transverse-shear deformation theory of reference 14. The buckling load determined by the first-order transverse-shear deformation theory is accurate to within a few percent compared to the higher-order theory and the added terms in the higher-order theory are not needed for isotropic cylinders.

3.1.2.2 Mildly Anisotropic Laminated Cylinders

Predicted buckling loads based on three theories are shown in figure 4 for $[\pm 45/90]_{ns}$ cylinders loaded in axial compression. The three theories are: 1) classical theory without transverse shear deformation; 2) the first-order transverse-shear deformation theory; and 3) the present higher-order shear deformation theory using assumed trigonometric or polynomial displacements in the thickness direction. The nondimensional parameters k_x, Z and s are based on material properties of isotropic

structures and are not directly applicable to laminated structures because laminated structures have different values of extensional stiffness and shear stiffness in each direction. Since the properties of laminated cylinders are not the same in all directions, a modified set of nondimensional parameters must be used. For laminated cylinders, D is replaced by $\sqrt{D_{11} \; D_{22}}$, Z is replaced by $L^2\sqrt{(12\ (1 - \mu_{12}\ \mu_{21}))}/(R\ t)$, and the thickness-to-length ratio t/L is specified instead of s, where D_{11}, and D_{22} are bending stiffnesses and μ_{12} and μ_{21} are the in-plane Poisson's ratios of the laminate. The parameter s is reduced to t/L by removing material properties and constants and taking the square root. Buckling loads for three values of t/L are presented in figure 4. The three curves have the same shape, though actual values of k_x and Z differ.

The in-plane material properties of Hercules Incorporated AS4-3502 graphite-epoxy unidirectional preimpregnated tape are assumed for the study (i.e., $E_l/E_t = 11.3$, $G_{lt}/E_t = .53$). The transverse properties assumed for the study are based on references 39 and 40 and are $G_{lz}/G_{lt} = 1.$, $G_{tz}/E_z = 1.$ and $G_{tz}/G_{lt} = .57$, (where l, t, and z represent the longitudinal, transverse and through-the-thickness directions of a 0-degree unidirectional laminate, respectively). Buckling loads for cylinders with a $[\pm 45/90]_{ns}$ laminate were determined for the three theories. The number of plies is assumed to be greater than 18 (more than 6 repetitions of ±45/90) so that the properties can be assumed to be transversely isotropic and anisotropic effects can be neglected.

For thin-walled cylinders (low values of Z) the buckling loads obtained from the three theories agree. For very short, thick-walled cylinders which buckle into very short wavelengths (cylinders with very large values of Z), the present theory agrees with the first-order transverse-shear deformation theory. For a limited range of Z between these two extremes, buckling loads are predicted by the present theory which are as much as 50 percent lower than those predicted by the first-order transverse-shear deformation theory as a result of including the additional terms to account for the effects of transverse shear deformation. In the range of Z where the theories give the same buckling load, the mode shapes at buckling are the same (the same pair of (m,n) give the minimum eigenvalue). In the range of Z where the predicted buckling loads are not the same (not within a few percent), the number of waves in the axial direction which gives the minimum eigenvalue is not the same for the first-order transverse-shear deformation theory as for the present theory. The buckling load calculations are based on the assumption that the buckling load occurs when the cylinder is being loaded in the elastic range. In some cases where the present theory predicts buckling loads which are significantly lower than predicted by the first-order theory, the strain in the cylinder at the predicted buckling load may be so large that the cylinder is no longer in the elastic range, in which case the bucking load predicted by either theory may be incorrect. Under those circumstances the cylinder may not buckle but may exhibit some other behavior. It should also be noted that the buckling loads predicted by the present higher-order theory have not been verified by experiment or by three-dimensional elasticity analysis.

Buckling loads of a $[\pm 45/90]_{ns}$ cylinder with $t/L = .05$ are shown in figure 5 for the first-order transverse-shear deformation and present theories with the number of half-waves in the axial direction at buckling shown at several points along the curve. The set of numbers above the curves are the number of half-waves at buckling predicted by the first-order transverse-shear deformation theory, the set below the curves are the number of half-waves predicted by the present theory. For $Z < 400$, the wave number increases consistently and steadily as Z increases for both theories. For $400 < Z < 5000$, the number of half-waves along the length of the cylinder predicted by the two theories differ significantly. As Z increases in this range, the first-order transverse-shear deformation theory's predictions of wave number continues to rise steadily until the maximum buckling load is reached and the wave number becomes very large. As Z increases above 400, the curve changes shape when the wave number at buckling predicted by the present theory changes. The wave number remains almost unchanged from $Z = 500$ to $Z = 2000$, then quickly rises again until the two predicted curves merge when short wavelength buckling is predicted at $Z \simeq 5000$.

3.1.2.3 <u>Orthotropic Laminated Cylinders</u>

Axial compressive buckling loads for cylinders with unidirectional 0-degree and 90-degree laminates and five values of t/L are shown in figures 6 and 7, respectively. The predicted buckling loads shown in these figures indicate that little reduction in buckling load below the predictions of first-order transverse-shear deformation theory occurs in cylinders with

unidirectional 0- and 90-degree laminates for any value of t/L. For thin-walled cylinders, the buckling load for cylinders with unidirectional 90-degree laminates is much lower than the buckling load for the cylinders with 0-degree laminates, but for thick-walled cylinders, there is very little difference in buckling loads. For example, the buckling load parameter k_x of a cylinder with a unidirectional 0-degree laminate, with $t/L = .1$ and $Z = 1$ is about 10 times that of the corresponding cylinder with a unidirectional 90-degree laminate; but the difference between the k_x for the two laminated cylinders with $Z = 1000$ is only a few percent. This difference in buckling loads predicted by the first-order transverse-shear deformation theory and by the present theory is no more than a few percent at any point on any of the curves. Even when a difference does occur, the difference occurs only in a limited range of Z. These figures resemble figure 3 for an isotropic cylinder more than figure 4 for a $[\pm 45/90]_{ns}$ laminated cylinder. The effect of the higher-order terms on predicted buckling loads is negligible for unidirectional $[0]_{ns}$ and $[90]_{ns}$ laminated cylinders.

3.1.3 Shear Correction Factors

3.1.3.1 Isotropic Cylinders

Shear correction factors have been used instead of higher-order terms to account for transverse-shear deformation effects on buckling loads. The traditional shear correction factor for isotropic materials is 5/6 (ref. 41). Buckling loads predicted by the first-order transverse-shear

deformation theory for metallic isotropic cylinders using a shear correction factor of 5/6 are presented in figure 8. The reduction in transverse shear stiffness has little effect on the buckling load except where the cylinder's buckling mode approaches and reaches short wavelength buckling. The buckling load at short wavelength buckling is strongly dependent upon the value of the shear moduli in the thickness direction (ref. 14). At short wavelength buckling the buckling load predicted by using the shear correction factor is slightly lower than the load predicted by the first-order transverse-shear deformation theory (without a shear correction factor) and the present higher-order theory since shear correction factors decrease the shear moduli.

3.1.3.2 Laminated Cylinders

The shear correction factor of 5/6 is only a first approximation of a shear correction factor which accounts for transverse shear deformation in the predicted buckling load of laminated cylinders. A better approximation uses a shear correction factor which takes into account the properties of the laminate used, such as laminate properties and stacking sequence. A method for calculating such shear correction factors is described in references 3 and 37. In reference 3 reductions larger than 5/6 in the transverse shear moduli are recommended for most laminates. The predicted buckling loads for $[\pm 45/90]_{ns}$ laminated cylinders are presented in figure 4 for the classical, first-order transverse-shear deformation, and present theories. These buckling loads for cylinders with geometries $t/L = .05$ as well as those predicted by the first-order transverse-shear deformation

theory with shear correction factors of 5/6 and those predicted by the procedure recommended in reference 3 are presented in figure 9. The predictions based on a shear correction factor of 5/6 agree with the higher-order theory better than the first-order transverse-shear deformation theory (with no shear correction factor) in the limited range of Z in which transverse shearing is important. Using a shear correction factor does not account for the change in buckling mode shape predicted at buckling by the higher-order theory discussed earlier. In the region of Z where the buckle pattern is short wavelength buckling, the prediction based on a shear correction factor of 5/6 is slightly lower than the buckling load predicted without a shear correction factor.

For large values of Z the buckling loads predicted by using a shear correction factor which takes into account laminate properties are slightly lower than those predicted by using a factor of 5/6. The difference between buckling loads predicted by first-order transverse-shear deformation theory (without a shear correction factor) and with a shear correction factor of 5/6 is larger than the difference between the loads predicted by using a factor of 5/6 and using the laminate shear correction factor. As with the shear correction factor of 5/6, the laminate shear correction factor reduces the predicted buckling load for the range of Z where the buckling mode approaches and reaches short wavelength buckling. The buckling load predicted by using the laminate shear correction factor is more accurate than the buckling load predicted by the first-order transverse-shear deformation theory in the limited range of Z where the higher-order theory demonstrates the most significant effects of transverse shearing. The use of a laminate shear correction factor with first-order transverse-shear deformation theory does not account for the change in mode shape predicted

by the higher-order theory using either polynomial or trigonometric higher order terms.

3.1.4 Effect of Stacking Sequence on Buckling Load

Parametric studies of the effects of stacking sequence on the axial compressive buckling load for thick-walled cylinders with $[\pm\theta/90]_{ns}$ and $[\pm\theta/0/90]_{ns}$ laminates are shown in figures 10 and 11. The buckling load parameter, k_x, is shown as a function of ply orientation, θ, for θ ranging from 0 to 90 degrees. Buckling loads predicted by the first-order transverse-shear deformation theory and by the present theory are shown in figure 10 for $[\pm\theta/90]_{ns}$ laminated cylinders and in figure 11 for $[\pm\theta/0/90]_{ns}$ laminated cylinders. Buckling loads for three cylinder geometries are presented in the figures. Two graphs are shown for each laminate because of the wide range of predicted buckling loads for the three geometries. The most significant effect of transverse shear deformation is for the geometries in which R/t is very small (i.e., 1.4) for either value of L/R.

Transverse shear deformation has little effect when θ is near 0 degrees or near 90 degrees, however its effect is significant for θ near 45 degrees for both types of laminated cylinders. The most significant decrease in buckling load is for $\theta = 45$ degrees, where a reduction in predicted buckling load of almost 50 percent occurs. The $[\pm45/0/90]_{ns}$ laminated cylinder is quasi-isotropic, but the low transverse shear modulus

causes the buckling load to decrease as it does for the $[\pm 45/90]_{ns}$ laminate and not as it does for the metallic isotropic laminated cylinder.

3.1.5 Buckling of Anisotropic Cylinders

Anisotropy can have a significant effect on the buckling load of laminated cylinders. Anisotropy interacts with boundary conditions and loading conditions so a measure of C_{16} and C_{26} alone is not adequate to evaluate the effects of anisotropy on a class of cylinders. The values of C_{16}, C_{26}, D_{16} and D_{26} provide an indication of the significance of anisotropy for the given loading and boundary conditions. These anisotropic material properties are expressed in nondimensional form in figure 12 for several mildly anisotropic and strongly anisotropic laminates. The four stacking sequences to be compared are symmetrically laminated and either balanced or consist only of 45-degree plies, so $C_{16} = C_{26}$ and $D_{16} = D_{26}$. The stacking sequences examined are $[\pm 45/0/90]_{4s}$, $[\pm 45/90]_{4s}$, $[\pm 45/90]_{1s}$, and $[45]_{2s}$. Each laminate is assumed to have the same total thickness and all plies within a laminate are assumed to be of equal thickness. The first two stacking sequences (those with subscript 4s) are mildly anisotropic. The value of D_{16}/D_{22} is very small. The last laminate listed, $[45]_{2s}$, is strongly anisotropic, with large values of C_{16}/C_{22} and D_{16}/D_{22}. Comparing the material properties is a good way of evaluating the relative importance of anisotropy in the laminates. In the study of buckling loads of mildly anisotropic and strongly anisotropic laminates which follows, only the effect of the material properties and cylinder geometries are examined. The

cylinders are assumed to be simply supported and subjected to axial compressive loadings.

3.1.5.1 Strongly Anisotropic Laminated Cylinders

A study of laminated angle-ply plates (ref. 26) shows that the ply orientations for which anisotropy has the most significant effect on buckling loads is 45 degrees and that the effect of anisotropy on buckling is insignificant in $[\pm 45/0/90]_{ns}$ laminated plates. The buckling loads for $[45]_{ns}$ laminated cylinders with a range of geometries predicted by four assumptions are shown in figure 13. The buckling loads for anisotropic cylinders are expressed using the same nondimensional parameters as for the orthotropic and isotropic cylinders. However, since these nondimensional parameters do not describe fully the stiffnesses in the cylinder, they have less significance for anisotropic cylinders than for orthotropic cylinders. The four assumptions are: 1) the first-order transverse-shear deformation theory with anisotropic effects neglected (i.e., $C_{16} = C_{26} = 0$); 2) the present theory with anisotropic effects neglected; 3) the first-order transverse-shear deformation theory with anisotropic effects included (i.e., C_{16} and C_{26} are not equal to 0); and 4) the present theory with anisotropic effects included. The first and second of these assumptions are represented by the solid curves. The third and fourth of these assumptions are represented by the dashed curves. The effect of anisotropy on the buckling load of laminated $[45]_{ns}$ cylinders is the difference between the two solid curves for first-order transverse-shear deformation theory, and between the

two dashed curves for the present theory. The effect of transverse shear deformation on the buckling load of laminated $[45]_{ns}$ cylinders is the difference between the upper solid and dashed curves for the assumptions in which anisotropic effects are neglected and between the lower solid and dashed curves for the assumptions in which anisotropic effects are included. The effect on the buckling load of more accurately accounting for transverse shear deformation is much less significant than the effect of accounting for anisotropy. In this case, a decrease in buckling load of 26 percent for the cylinder with $R/t = 10$ results from including the effects of anisotropy but a decrease in buckling load of only a few percent results from including transverse-shear deformation effects.

The first-order transverse-shear deformation and present theories predict the buckling loads in figure 4 if anisotropic effects are neglected. Predicted buckling loads for which anisotropic effects are included for the $[\pm 45/0/90]_{ns}$ and $[\pm 45/90]_{ns}$ laminated cylinders are not presented in this report because the reduction in buckling load due to the effect of anisotropy is less than 1 percent of the buckling load for all geometries studied.

3.1.5.2 Sensitivity to Anisotropic Effects

The sensitivity parameter, ρ, as defined in Appendix A, is an indicator of the significance of anisotropic effects on buckling loads. Buckling loads of cylinders which have a large value of $|\rho|$ are strongly dependent on anisotropic effects. A positive value of ρ indicates that the buckling load of the cylinder is increased by including anisotropic

effects and a negative value of ρ indicates that the buckling load is decreased by including anisotropic effects. The sensitivity parameter is indicated on plots of buckling load as a function of Z for several cylinders with two stacking sequences in figure 14. The solid lines and square symbols represent the $[45]_{ns}$ laminated cylinders and the dashed line and diamond symbols represent the $[\pm 45/90]_{ns}$ laminated cylinders. The orthotropic and anisotropic solutions for the $[\pm 45/90]_{ns}$ cylinders are the same so only one dashed line is shown.

Four sets of cylinder dimensions, represented by the data points, are presented in figure 14. The geometries were chosen to produce values of Z which represent each section of the curve of the k_x versus Z plots shown in figures 3 and 13. The values of Z examined are approximately 1, 100, 1000, and 10,000. The magnitudes of ρ at each of these points on the k_x versus Z curve for cylinders of the two stacking sequences are shown in figure 14. The effect of anisotropy is far more significant for all points examined for the $[45]_{ns}$ laminated cylinder than the $[\pm 45/90]_{ns}$ laminated cylinder.

For the cylinder with $Z \approx 1$, the difference between the buckling loads predicted by including and by neglecting anisotropic effects is 9.1 percent for the $[45]_{ns}$ laminated cylinder and less than .1 percent for the $[\pm 45/90]_{ns}$ laminated cylinder. This difference corresponds to magnitudes of $|\rho|$ equal to .14 and .002, respectively. In this section of the k_x versus Z curve, the dependence on anisotropy is relatively small even for the $[45]_{ns}$ laminated cylinder. For $Z \approx 100$, including the effects of

anisotropy reduces the predicted buckling load by 26 percent and .003 percent for the two types of cylinders. This difference corresponds to magnitudes of $|\rho|$ equal to .22 and .002, respectively. The effect of anisotropy on the predicted buckling load is significant for the $[45]_{ns}$ laminated cylinders for $Z \simeq 100$. For $Z \simeq 1000$, the difference between buckling loads predicted by neglecting and by including anisotropy is 55 percent and .1 percent, respectively. For short wavelength buckling, i.e, $Z \simeq 10{,}000$, the effect of anisotropy is negligible for both laminated cylinders. For short wavelength buckling, $|\rho| < .001$ for the $[\pm 45/90]_{ns}$ cylinders and $|\rho| < .00001$ for the $[45]_{ns}$ cylinders.

Using the method described in Appendix A, an approximate buckling load for the anisotropic cylinder can be found from equation (A.10) and repeated here as equation (21)

$$\bar{k}_x \simeq k_x \, (1 + \rho) \tag{21}$$

where $\bar{k}_x$ is the approximate buckling load of the anisotropic cylinder. The nondimensional parameter $\bar{k}_x$ is based on the buckling load parameter, k_x, calculated by neglecting anisotropic effects, and on the sensitivity parameter, ρ.

Since the calculated value of ρ is less than zero, the buckling load approximation for the anisotropic cylinder is less than the buckling load predicted by neglecting anisotropy. The accuracy of equation (20) can be evaluated from an example based on a data point in figure 14.

For the laminated $[45]_{ns}$ cylinder with $Z \simeq 1000$, $\rho = -.424$ and $k_x = 169$. Using the formula in equation (20), $\bar{k}_x = 98$. This value of $\bar{k}_x$ is a very good approximation of the value of k_x at $Z \simeq 1000$ on the solid curve labeled anisotropic. Only the first two terms in the Taylor series expansion are needed to predict accurate buckling loads of the anisotropic cylinder.

3.2 Combined Loads

The interaction between axial compression N_x and external pressure P ($N_\theta = P\ R$) loadings for isotropic cylinders and laminated cylinders of four stacking sequences is shown in figures 15-19. These loadings are shown on the figures as N_x applied to the ends of the cylinder and P applied to the entire wall of the cylinder as shown in a typical section of the cylinder wall. Buckling loads predicted by two transverse-shear deformation theories, first-order transverse-shear deformation theory and the present higher-order transverse-shear theory, are shown for cylinders with radius-to-thickness ratios of 10 and 1.4 and length-to-thickness ratios of 1 and 14.3, respectively.

Since transverse-shear deformation effects cause little reduction in the axial compressive buckling loads of isotropic and unidirectional 0- and 90-degree laminates, little difference in the interaction curves for these cylinders is expected. There is virtually no effect on the buckling load predicted by adding higher-order terms to account for transverse shearing for either geometries of isotropic cylinders subjected to axial compressive

and external pressure loadings. The buckling load results for the two methods are indistinguishable for aluminum cylinders, as shown in figure 15, because one curves lies on top of the other.

No difference in the buckling load results is detectable for the unidirectional laminated cylinders of $[0]_{ns}$ or $[90]_{ns}$ for $R/t = 10$ and $L/R = 1$, as shown in figure 16. A small reduction in buckling load can be seen for these two laminates for cylinders with geometries $R/t = 1.4$ and $L/R = 14.3$, as shown in figure 17. As in the case of axial compressive loadings alone, the addition of higher-order terms has a negligible effect on the buckling load predictions for unidirectional $[0]_{ns}$ and $[90]_{ns}$ laminated cylinders.

Buckling loads predicted by the two theories for laminated cylinders of $[\pm 45/90]_{ns}$ and $[\pm 45/0/90]_{ns}$ stacking sequences for the same cylinder dimensions as above are shown in figures 18 and 19. Little difference in buckling load results can be seen in figure 18 for either laminate with $R/t = 10$. However, the laminated cylinders of $R/t = 1.4$ which contain 45-degree plies have predicted buckling loads which are significantly reduced by including the higher-order terms, as shown in figure 19.

CHAPTER IV

CONCLUDING REMARKS AND RECOMMENDATIONS FOR FUTURE RESEARCH

4.1 Summary

An analytical study of the effects of transverse shear deformation and anisotropy on the buckling loads of orthotropic and anisotropic laminated cylinders subjected to axial compression and/or external pressure loads was conducted. The effects on buckling loads of adding higher-order terms to the displacement series of classical shell buckling theories were studied. Buckling loads predicted by classical theory, first-order transverse-shear deformation theory and the higher-order theory were compared to determine which cylinder geometries and laminate stacking sequences have a reduction in buckling load due to transverse shearing. These results were also compared to buckling loads predicted by using the first-order transverse-shear deformation theory with shear correction factors. A parametric study of buckling loads of cylinders with $[\pm\theta/90]_{ns}$ and $[\pm\theta/0/90]_{ns}$ laminates was conducted to determine which laminates are most sensitive to transverse-shear deformation effects. Anisotropic effects were studied by comparing buckling loads predicted by the first-order transverse-shear deformation theory and by the higher-order theory with anisotropic material properties neglected and with anisotropic material properties included.

4.2 Conclusions

Trigonometric and polynomial terms in the thickness direction were added to the displacement terms used in the first-order transverse-shear deformation theory to obtain two forms of the higher-order theory. For the range of parameters considered, the addition of one trigonometric or one polynomial term in each displacement direction leads to equal reductions of predicted buckling loads. The addition of more than one term in each displacement direction does not lead to further reductions in the predicted buckling load for either polynomial or trigonometric displacement terms.

Buckling loads predicted by the higher-order theory based on consistent assumed strain-displacement relations and based on inconsistent assumed strain-displacement relations were calculated for laminated cylinders loaded in axial compression. These strain-displacement relations lead to compatibility equations which are valid and invalid, respectively. Buckling load predictions based on the consistent and inconsistent assumptions for cylinders of moderately thick and very thick walls are significantly different. The buckling loads based on the inconsistent assumptions in the linear and nonlinear parts of the strain-displacement relations are much lower than the buckling loads based on the consistent assumptions.

For isotropic cylinders and for unidirectional $[0]_{ns}$ and $[90]_{ns}$ laminated cylinders, little accuracy appears to be gained by adding the complication of trigonometric or polynomial terms in the thickness direction for all cylinder geometries studied. The difference between buckling loads predicted by the first-order transverse-shear deformation theory and by the higher-order theory is very small for most geometries of laminated cylinders

of any stacking sequence studied. However, for some short laminated cylinders with thick walls and ply orientations near 45 degrees, the addition of higher-order terms appears to cause a significant reduction in predicted buckling loads to values below those determined by the first-order transverse-shear deformation theory. There seems to be a limited range of cylinder geometries in which the addition of higher-order terms to account for transverse shearing leads to predicted buckling loads which are as much as 50 percent lower than the buckling loads predicted by the first-order transverse-shear deformation theory for $[\pm 45/90]_{ns}$ laminated cylinders. This limited range includes cylinders with dimensions such that $R/t \simeq 1.4$ and $L/R \simeq 14$. For the limited range of cylinder geometries between low values of Z and very high values of Z, the buckling loads predicted by the first-order transverse-shear deformation theory are significantly higher than the buckling loads predicted by the higher-order theory.

For this limited range of cylinder geometries, the use of shear correction factors provides a simple way of finding buckling loads which are between those predicted by the first-order transverse-shear deformation theory and those predicted by the present higher-order theory. The use of shear correction factors with the first-order transverse-shear deformation theory does not predict the same buckling load or mode shape as the higher-order theory but it is an improvement over the first-order transverse-shear deformation theory without shear correction factors.

A parametric study of stacking sequences of the form $[\pm\theta/90]_{ns}$ and $[\pm\theta/0/90]_{ns}$ seems to indicate that the amount of reduction in buckling load due to transverse shearing is dependent upon the stacking sequence. The addition of higher-order terms to the displacement series seems to have a

negligible effect on the predicted buckling loads for θ near 0 degrees and near 90 degrees for both types of laminates. However, for θ near 45 degrees, the buckling loads predicted by the present theory can be as much as 50 percent below the buckling loads predicted by the first-order transverse-shear deformation theory.

The effect of anisotropy on the bucking loads of strongly anisotropic laminated cylinders, such as a $[45]_{ns}$ laminate, appears to be more important than the transverse-shearing effects for all the cylinder geometries examined in this study. Anisotropic properties have a significant effect on predicted buckling loads of a wide range of cylinder geometries. Neglecting the anisotropic effects in a strongly anisotropic cylinder leads to non-conservative errors in the predicted buckling loads.

The effect of the interaction of axial compressive and external pressure loadings on the buckling of isotropic, $[0]_{ns}$, $[90]_{ns}$, $[\pm 45/90]_{ns}$, and $[\pm 45/0/90]_{ns}$ cylinders was studied. The differences between buckling loads predicted by the first-order theory and by the present theory are negligible for all geometries of isotropic cylinders studied when subjected to combined loads. For laminated cylinders, the reduction in predicted buckling loads due to including the higher-order terms in the assumed displacement series is only apparent for very thick-walled, short cylinders. In the case of combined loads, as well as with axial compressive loadings alone, the buckling loads of unidirectional $[0]_{ns}$ and $[90]_{ns}$ laminated cylinders are not significantly reduced by including the higher-order terms. However, the predicted buckling loads of $[\pm 45/90]_{ns}$ and $[\pm 45/0/90]_{ns}$ laminated cylinders are significantly lower

for the present theory than for the first-order transverse-shear deformation theory.

The following conclusions can be drawn from the results of this investigation:

(1) Classical theory is adequate for predicting buckling loads for all types of cylinders studied which have walls which are thin or moderately thick (low or moderate values of the curvature parameter Z) when subjected to axial compressive loading for all cylinder geometries and boundary conditions studied.

(2) The first-order transverse-shear deformation theory is adequate for predicting buckling loads for isotropic and unidirectional $[0]_{ns}$ and $[90]_{ns}$ cylinders subjected to axial compression for all cylinder geometries and boundary conditions studied (all values of Z). The first-order transverse-shear deformation theory is also adequate for predicting buckling loads for very thick-walled (high values of Z) laminated cylinders which buckle into very short waves.

(3) For cylinders with moderate or high values of Z, the use of shear correction factors leads to buckling loads which are lower than those predicted by the first-order transverse-shear deformation theory but not as low as predicted by the higher-order theory.

(4) The addition of one trigonometric or polynomial term in the thickness direction in each assumed displacement series leads to the same predicted buckling load so neither series is superior to the other in making accurate predictions.

(5) Consistent assumptions in the linear and nonlinear terms in the strain-displacement relations which do not violate the compatibility requirements are required to obtain accurate buckling loads from the higher-order theory.

(6) Higher-order terms appear to be needed to account for the reduction in buckling loads due to transverse shearing for cylinders in the limited range of cylinder geometries between moderate values of Z and very high values of Z.

(7) A parametric study of stacking sequences of the form $[\pm\theta/90]_{ns}$ and $[\pm\theta/0/90]_{ns}$ seems to indicate that the laminated cylinders whose axial compressive buckling loads are most affected by transverse shearing are those containing 45-degree plies.

(8) The magnitude of the buckling load is more sensitive to anisotropic effects than to transverse-shear deformation effects for strongly anisotropic cylinders.

(9) The addition of higher-order terms through the thickness reduces the predicted buckling loads of cylinders subjected to external pressure loadings by approximately the same percent as the reduction in predicted buckling loads of cylinders subjected to axial compressive loadings.

4.3 Recommendations for Future Research

This work on cylindrical shell buckling could be extended in many ways. Boundary conditions other than simple support could be considered. Shear loading alone or with axial compression and external pressure could be considered. Initial geometric imperfections or stiffeners could be included

in the cylinders. On a broader outlook, the present theory could be applied to other types of shells or extended into the postbuckling load range. Experimental results would also be useful as a means of verifying the analytical results presented.

Future research could include conducting experiments that involve loading thick-walled laminated graphite-epoxy cylinders in axial compression until buckling. Several types of materials and stacking sequences could be studied to compare experimental results and to determine which laminates are most affected by transverse shearing. A comparison could also be made to see if the experimental results agree with the analytical ones.

APPENDIX A

DEVELOPMENT OF SENSITIVITY PARAMETER

Parameters which can be used to evaluate the sensitivity of the buckling load of a laminated panel to anisotropic material coefficients are developed in reference 25. The method used in reference 25 can be applied to laminated cylinders to evaluate their sensitivity to anisotropic material coefficients. These sensitivity parameters give a relative indication of how significant the effects of anisotropy are on the buckling load of cylinders. The higher the magnitude of the sensitivity parameter, the more significant the effect of anisotropy on the buckling load of the cylinder.

Sensitivity parameters for cylinders subjected to axial compressive loadings are calculated by starting with the eigenvalue problem presented in equation (20), rewritten as equation (A.1) by substituting $\{x\}$ as the displacement vector and Ω as the eigenvalue of the anisotropic problem.

$$[K]_{ANISO} \{x\} = \Omega \, [B_1]_A \{x\} \tag{A.1}$$

In reference 25, the matrix $[K]_{ANISO}$ is decomposed into two matricies, each with the same dimensions as the original matrix. The first of these two matricies, $[K]_o$, contains only the orthotropic terms from $[K]_{ANISO}$. The matrix $[K]_o$ is a block diagonal matrix in which each block matrix is associated with one value of wave number in the longitudinal direction, m_i. The second of the two matricies, $[K]_a$, contains all the non-orthotropic

terms from $[K]_{ANISO}$ (all of the C_{16} and C_{26} terms). The matrix $[K]_a$ has block matricies of zero and non-zero terms. Each block matrix is associated with a pair of longitudinal wave numbers, m_i and m_j. The matricies $[K]_o$ and $[K]_a$ are shown in equations (A.2) for a problem in which three consecutive values of longitudinal wave number m_i where $i=1,2,3$ are used.

$$[K]_o = \begin{bmatrix} [\ f(m_1)\ ] & [\ 0\ ] & [\ 0\ ] \\ [\ 0\ ] & [\ f(m_2)\ ] & [\ 0\ ] \\ [\ 0\ ] & [\ 0\ ] & [\ f(m_3)\ ] \end{bmatrix}$$

$$[K]_a = \begin{bmatrix} [\ 0\ ] & [f(m_1,m_2)] & [\ 0\ ] \\ [f(m_2,m_1)] & [\ 0\ ] & [f(m_3,m_2)] \\ [\ 0\ ] & [f(m_2,m_3)] & [\ 0\ ] \end{bmatrix} \tag{A.2}$$

In the matrix of orthotropic terms, each diagonal block matrix is based on only one value of m_i and corresponds to the $[K]$ matrix in equation (10). In the matrix of anisotropic terms, each off-diagonal block matrix is based on two different values of m_i. The orthogonality of the displacement series shown in equation (20) causes all block matricies which are dependent upon the combinations of m_i and m_j such that $j=i$ or $j=i+2$ to be [0]. The orthogonality also causes block matricies which are dependent upon the combinations of m_i and m_j such that $j=i+1$ to be non-zero block

matricies. The relationship between $[K]_o$, $[K]_a$, and $[K]_{ANISO}$ is shown in equations (A.3).

$$[K]_o + \lambda [K_a] = [K]_{ANISO} \tag{A.3}$$

$$\lambda = 1.$$

The tracing parameter λ is a marker to indicate whether anisotropic effects are included (λ=1) or neglected (λ=0).

When equation (A.3) is substituted into equation (A.1) and λ=0, the eigenvalues are the orthotropic cylinder buckling loads. To find the sensitivity parameter, the orthotropic cylinder buckling loads must be known, and are found from equation (10) for each longitudinal wave number (3 in this case), or from equation (A.4). When λ=0, Ω is the eigenvalue for the orthotropic problem.

$$[K]_{ANISO} \{x\} = \Omega [B_1]_A \{x\} \tag{A.4}$$

$$\lambda = 0$$

The sensitivity parameter, ρ, is developed in reference 25 and defined in equation (A.5).

$$\rho = \partial^2\Omega/\partial\lambda^2 \; / \; (2 \; \Omega) \tag{A.5}$$

Derivatives of Ω with respect to λ are evaluated by using equations (A.6). Details of the derivation are presented in reference 25.

$$([K]_o - \Omega [B]_T) \{\partial x/\partial\lambda\} + \lambda [K]_a \{\partial x/\partial\lambda\} - \partial\Omega/\partial\lambda \; [B]_T\{x\} = - [K]_a \{x\}$$

$$([K]_o + \Omega [B]_T) \{\partial^2 x/\partial\lambda^2\} + [K]_a\{\partial x/\partial\lambda\} + \lambda [K]_a\{\partial^2 x/\partial\lambda^2\} \tag{A.6}$$

$$- \partial^2\Omega/\partial\lambda^2 [B]_T \{x\} - \partial\Omega/\partial\lambda [B]_T \{\partial x/\partial\lambda\} = - [K]_a \{\partial x/\partial\lambda\}$$

where $\{\partial^2\Omega/\partial\lambda^2\}$ is found by evaluating the second equation of (A.6) at $\lambda=0$, and by taking into account that $\partial\Omega/\partial\lambda = \{x\}^t [K]_a \{x\} = 0$ because of the form of the zero and non-zero blocks in $[K]_a$.

There will be one Ω and one $\partial\Omega^2/\partial\lambda^2$ for each value of m_i assumed. The minimum Ω when $\lambda=0$ is the orthotropic buckling load of the cylinder. The ρ associated with that Ω is the anisotropic sensitivity parameter of the cylinder. In general, $\rho < 0$ and a lower predicted buckling load will result from including the anisotropic effects than from neglecting them.

The anisotropic sensitivity parameter is evaluated to determine the importance of anisotropy to the buckling load of a cylinder. For a truly orthotropic cylinder, ρ is equal to zero. For a mildly anisotropic cylinder, $|\rho|$ is less than .1. For a strongly anisotropic cylinder, $|\rho|$ is greater than .25 (as defined in reference 25).

The anisotropic sensitivity parameter, ρ, can be used to find an approximation of the buckling load of the anisotropic cylinder without calculating the eigenvalue of the problem presented in equation (A.3) which includes both the anisotropic and orthotropic terms. This approximation is calculated from the buckling load found by neglecting anisotropy (the solution to equation (A.4)) and the sensitivity parameter, ρ. This method provides a way of accounting for anisotropy but avoids solving the large eigenvalue problem of equation (20).

A Taylor series expansion as shown in equation (A.7) can be used to approximate the buckling load of the anisotropic cylinder.

$$\Omega\big|_{\lambda=1} = \Omega\big|_{\lambda=0} + \frac{\lambda^2}{2!}\frac{\partial^2\Omega}{\partial\lambda^2} + \ldots \tag{A.7}$$

For simplification, let $\omega = \Omega\big|_{\lambda=0}$ which leads to $\frac{\lambda^2}{2!}\frac{\partial^2\Omega}{\partial\lambda^2} = \rho\,\omega$. These quantities have been found using equations (A.4) and (A.5), respectively.

By using only the first two terms in the Taylor series expansion, equation (A.8) results.

$$\Omega\big|_{\lambda=1} \simeq \omega\,(1 + \rho) \tag{A.8}$$

Converting the buckling loads in equation (A.8) to nondimensional parameters involving k_x, the nondimensionalized buckling load approximation, $\bar{k}_x$, can be expressed as:

$$\bar{k}_x \simeq k_x\,(1 + \rho) \tag{A.9}$$

REFERENCES

1. Timoshenko, S. P.: "On the Correction for Shear of the Differential Equation for Transverse Vibrations of Prismatic Bars." Philosophical Magazine, vol. 41, 1921, pp. 744-746.

2. Stavsky, Y.; and Friedland, S.: "Stability of Heterogenous Orthotropic Cylindrical Shells in Axial Compression." Israel Journal of Technology, vol. 7, no. 1-2, 1969, pp. 111-119.

3. Dong, S. B.; and Tso, F. K.: "On Laminated Orthotropic Shell Theory Including Transverse Shear Deformation." Journal of Applied Mechanics, vol. 39, 1972, pp. 1091-1096.

4. Levinson, M.: "An Accurate Simple Theory of the Statics and Dynamics of Elastic Plates." Mechanics Research Communications, vol. 7, 1980, pp. 343-350.

5. Reissner, E.: "A Twelfth Order Theory of Transverse Bending of Transversely Isotropic Plates," Zeitschrift Für Angewandte Mathematik und Mechanik, vol. 63, 1983, pp. 285-289.

6. Reddy, J. N.: "A Simple Higher-Order Theory for Laminated Composite Plates." Journal of Applied Mechanics, vol. 51, December 1984, pp. 745-752.

7. Kan, A.; and Kaplan, B.: "Calculation of Inhomogeneous Cylindrical Shells Taking into Account of Transverse Shear and Fiber Contraction." Soviet Applied Mechanics, vol. 15, no. 1, July 1979, pp. 26-32.

8. Anon.: "Buckling of Thin-walled Circular Cylinders." NASA SP-8007, August 1968.

9. Batdorf, S. B.: "A Simplified Method of Elastic-Stability Analysis for Thin Cylindrical Shells." NACA Report 874, 1947.

10. Simitses, G. J.; Sheinman, I.; and Shaw, D.: "The Accuracy of Donnell's Equations for Axially-Loaded, Imperfect Orthotropic Cylinders." Computers and Structures, vol. 20, no. 6, 1985, pp. 939-945.

11. Kobayshi, S.; Kayama, K.; Seko, H.; and Hirose, K.: "Compressive Buckling of Graphite-Epoxy Composite Circular Cylindrical Shells." Progress in Science and Engineering of Composites, vol. 1, 1982, pp. 555-564.

12. Mah, G. B.; Almroth, B. O.; and Pittner, E. V.: "Buckling of Orthotropic Cylinders," AIAA Journal, vol. 6, no. 4, April 1968, pp. 598-602.

13. Vasil'ev, V. V.: "Theory of Composite Shells." Mechanics of Composites, Mir Publishers, Moscow, 1982, pp 223-251.

14. Stein, Manuel; and Mayers, J.: "Compressive Buckling of Simply

Supported Curved Plates and Cylinders of Sandwich Construction." NACA TN 2601, January 1952.

15. Cohen, Gerald: "Buckling of Laminated Anisotropic Shells Including Transverse Shear Deformation." Computer Methods in Applied Mechanics and Engineering, vol. 26, 1981, pp. 197-204.

16. Levy, M.: "Memoire Sur la Theorie des Plaques Elastiques Planes." Journal Mathematiqués, Pur et Appliqué, vol. 3, 1887, pp. 219-306.

17. Stein, Manuel: "Nonlinear Theory for Laminated and Thick Plates and Shells Including the Effects of Transverse Shearing." Proceedings of the 26th AIAA/ASME/ASCE/AHS Structures, Structural Dynamics and Materials Conference, AIAA Paper No. 85-0671-CP, April 1985.

18. Stein, Manuel: "Nonlinear Theory for Thick Plates and Shells Including the Effects of Transverse Shearing," AIAA Journal, vol. 24, no. 9, September 1986, pp. 1537-1541.

19. Dittoe, F. A.; and Dharmarijan, S.: "Buckling of Eccentrically Stiffened Orthotropic Cylinders Under Combined Axial, Circumferential and Torsional Loading." Proceedings of the 9th AIAA/ASME Structures, Structural Dynamics and Materials Conference, AIAA Paper No. 68-293, 1968.

20. Tennyson, R. C.; Booton, M.; and Hui, D.: "Changes in Cylindrical Shell Buckling Behavoir Resulting from System Parameter Variation." Theoretical and Applied Mechanics; Proceedings of the 15th International Congress, 1980, pp. 417-430.

21. Onoda, Junjiro: "On the Laminate Configurations which Maximize the Buckling Loads of Composite Circular Cylinders." Proceedings of the 26th AIAA/ASME/ASCE/AHS Structures, Structural Dynamics and Materials Conference, 1985, pp. 690-696.

22. Uemura, M; and Kasuya, H.: "Coupling Effect on Axial Compressive Buckling of Laminated Composite Cylindrical Shells." Progress in Science and Engineering of Composites, Proceedings of the 4th International Conference on Composite Materials, 1982, pp. 583-590.

23. Tennyson, R. C.; and Hansen, J. S.: "Optimum Design for Buckling of Laminated Cylinders." Collapse: The Bucking of Structures in Theory and Practice, Proceedings of the IUTAM Symposium, 1982, pp. 409-429.

24. Zitzenanoch, L. D.: "Designing Graphite Cylinders to Resist Buckling." Proceedings of the 21st AIAA/SAE/ASME/ASEE Joint Propulsion Conference, AIAA Paper No. 85-1101, July 1985.

25. Noor, Ahmed K.; and Whitworth, Sandra L.: "Model Size Reduction for Buckling and Vibration Analyses of Anisotropic Panels." Journal of Engineering Mechanics, vol. 113, no. 2, February 1987, pp. 170-185

26. Nemeth, Michael P.: "Importance of Anisotropy on Buckling of Compression-Loaded Symmetric Composite Panels." AIAA Journal, vol. 24, no. 11, November 1986, pp. 1831-1835.

27. Dong, S. B.; Pister, K. S.; and Taylor, R. L.: "On the Theory of Laminated Anisotropic Shells and Plates." Journal of Aerospace Sciences, vol. 29, 1962, pp. 969-975.

28. Leissa, Arthur W.: "A Review of Laminated Composite Plate Buckling." Applied Mechanics Review, vol. 40, no. 5, May 1987, pp. 575-591.

29. Leissa, Arthur W.: "Buckling of Laminated Composite Plates and Shell Panels." AFWAL-TR-85-3069, June 1985.

30. Tennyson, R. C.: "Interaction of Cylindrical Shell Buckling Experiments with Theory." Theory of Shells, North-Holland Publishing Company, 1980, pp. 65-116.

31. Tennyson, R. C.; and Muggeridge, D. B.: "Buckling of Laminated Anisotropic Imperfect Circular Cylinders Under Axial Compression." Proceedings of the 10th AIAA Aerospace Sciences Meeting, AIAA Paper No. 72-139, 1972.

32. Tasi, J.; Feldman, A.; and Stang, D. A.: "The Buckling Strength of Filament-Wound Cylinders Under Axial Compression." NASA CR 266, July 1965.

33. Harris, L. A.; Suer, H. S.; and Skene, W. T.: "The Stability of Thin-Walled Unstiffened Circular Cylinders under Axial Compression Including the Effects of Internal Pressure." Journal of Aeronautical Sciences, August 1957, vol. 24, no. 8, pp. 587-596.

34. Novozhilov, V. V.: Foundations of the Nonlinear Theory of Elasticity, Graylock Press, 1953, Rochester, New York.

35. Ward, R. C.: "An Extension of the QZ Algorithm for solving Generalized Matrix Eigenvalue Problems." NASA TN D-7305, July, 1973.

36. Timoshenko, S. P.; and Goodier, J. N.: Theory of Elasticity, third edition, McGraw-Hill, 1951.

37. Noor, A. K.: "Stability of Multilayered Composite Plates." Fibre Science and Technology, vol. 8, no. 2, April 1975, pp. 81-89.

38. Reddy, J. N.: "Exact Solutions of Moderately Thick Laminated Shells." Journal of Engineering Mechanics, ASCE, vol. 110, 1984, pp. 794-809.

39. Seide, Paul; and Chang, Peter N.-H.: "Finite Element Analysis of Laminated Plates and Shells, volume 1, Annual Progress Report," March 1977 - March 1978, also available as NASA CR 157106, March 1978.

40. Rubben, A.; and Scharr, G.: "Method to Determine the Complete Three-dimensional Elastic Compliance Matrix of Composite Materials," Composite Structures, vol. 3, 1985, pp. 760-773.

41. Reissner, E.: "The Effect of Transverse Shear Deformation on the Bending of Elastic Plates," Journal of Applied Mechanics, vol. 12, no. 2, June 1945, pp. 69-77.

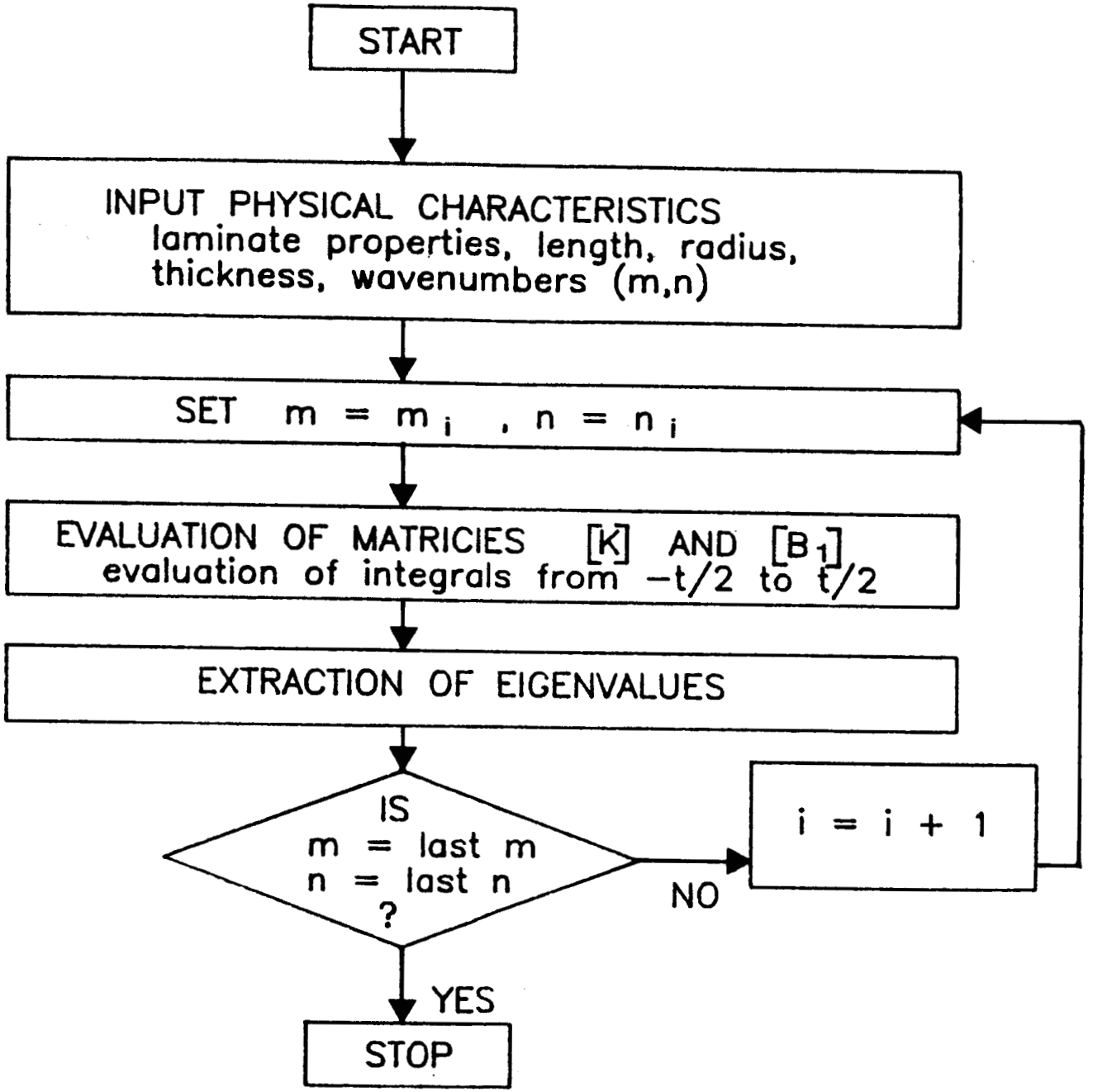

Figure 1. Flow chart of computer code which calculates buckling loads of orthotropic cylinders.

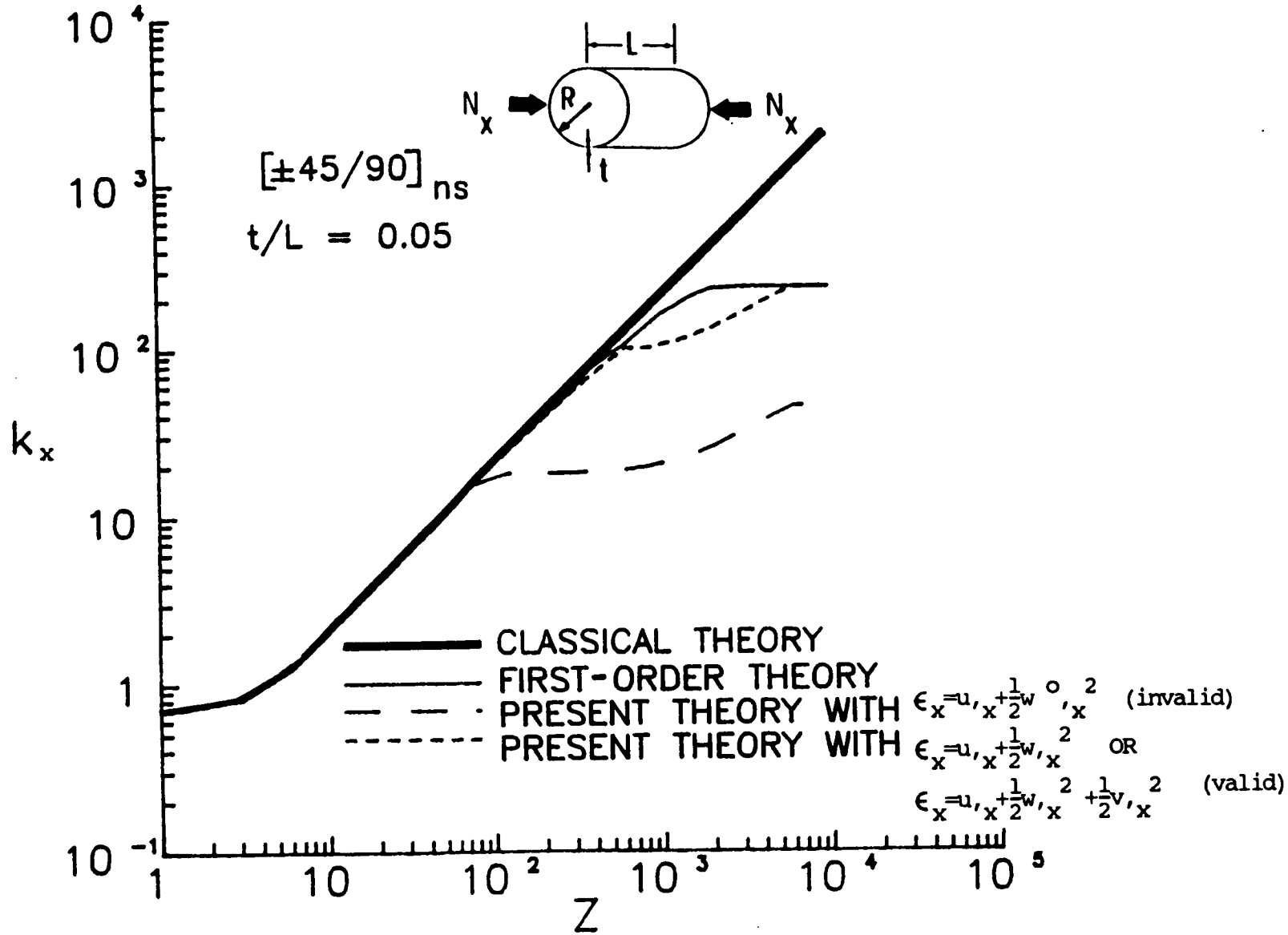

Figure 2. Importance of consistency and compatibility of assumed strains in calculating buckling loads.

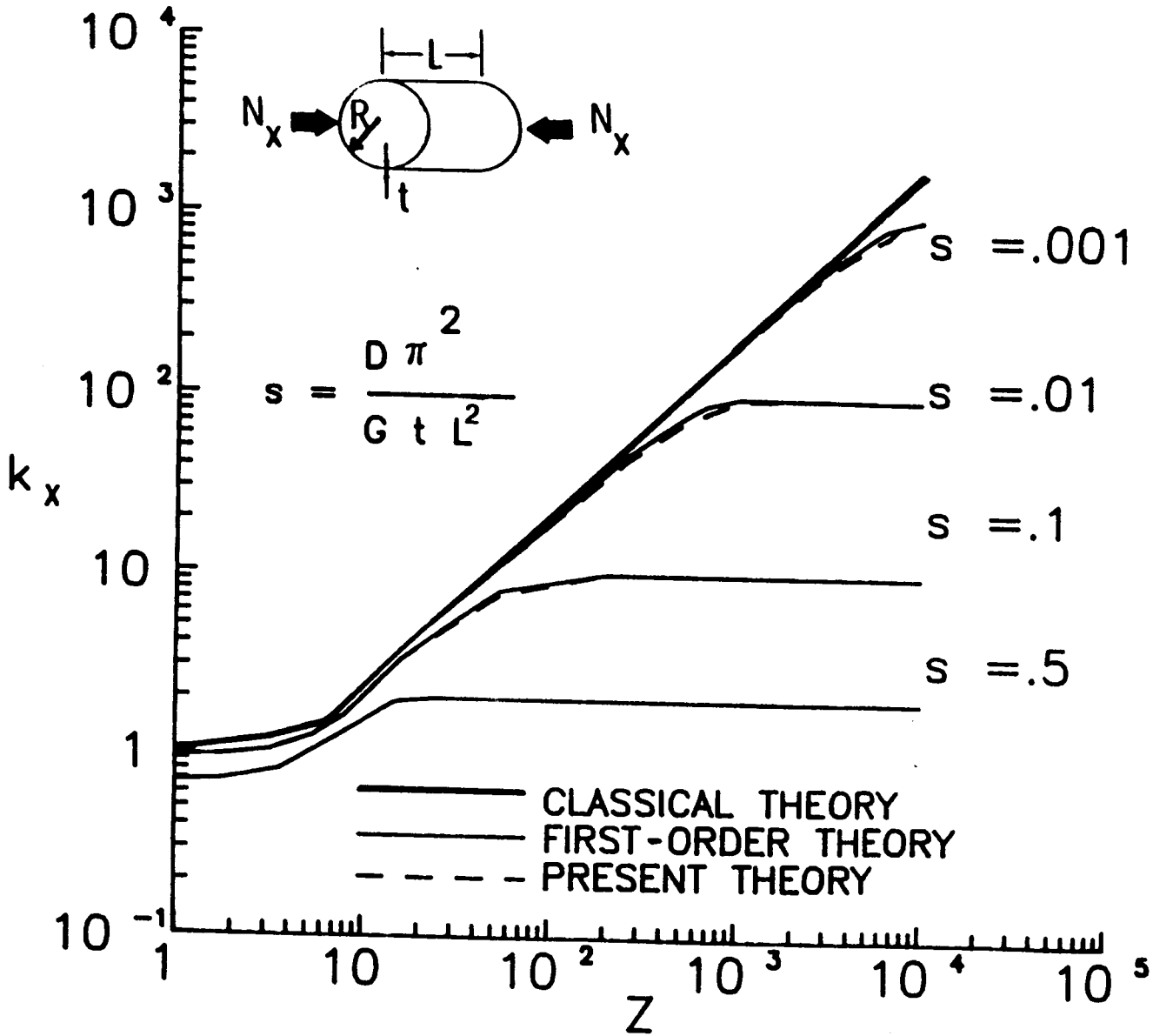

Figure 3. Effect of transverse shear deformation on axial compressive buckling loads of isotropic cylinders.

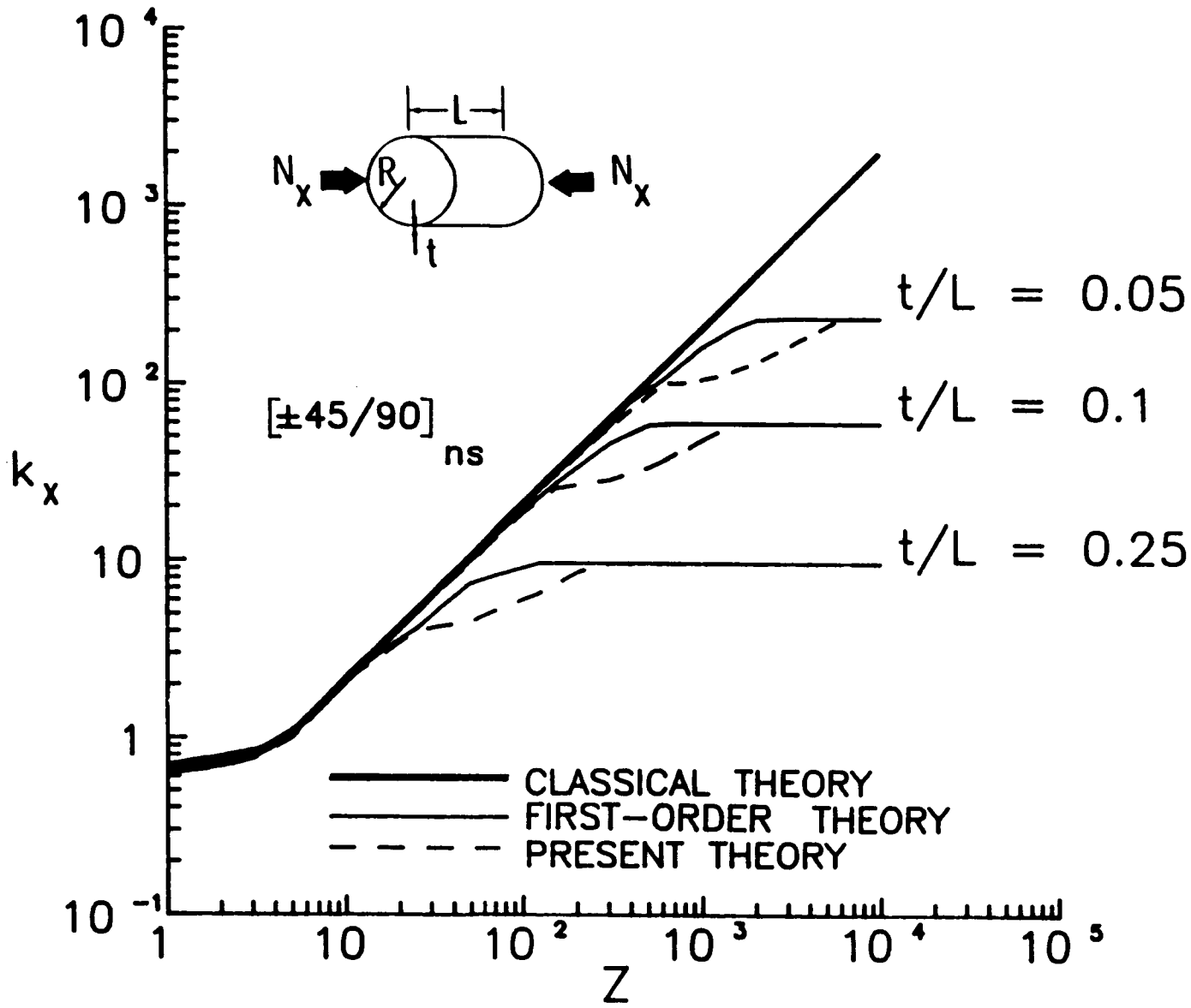

Figure 4. Effect of transverse shear deformation on axial compressive buckling loads of $[\pm 45/90]_{ns}$ laminated cylinders.

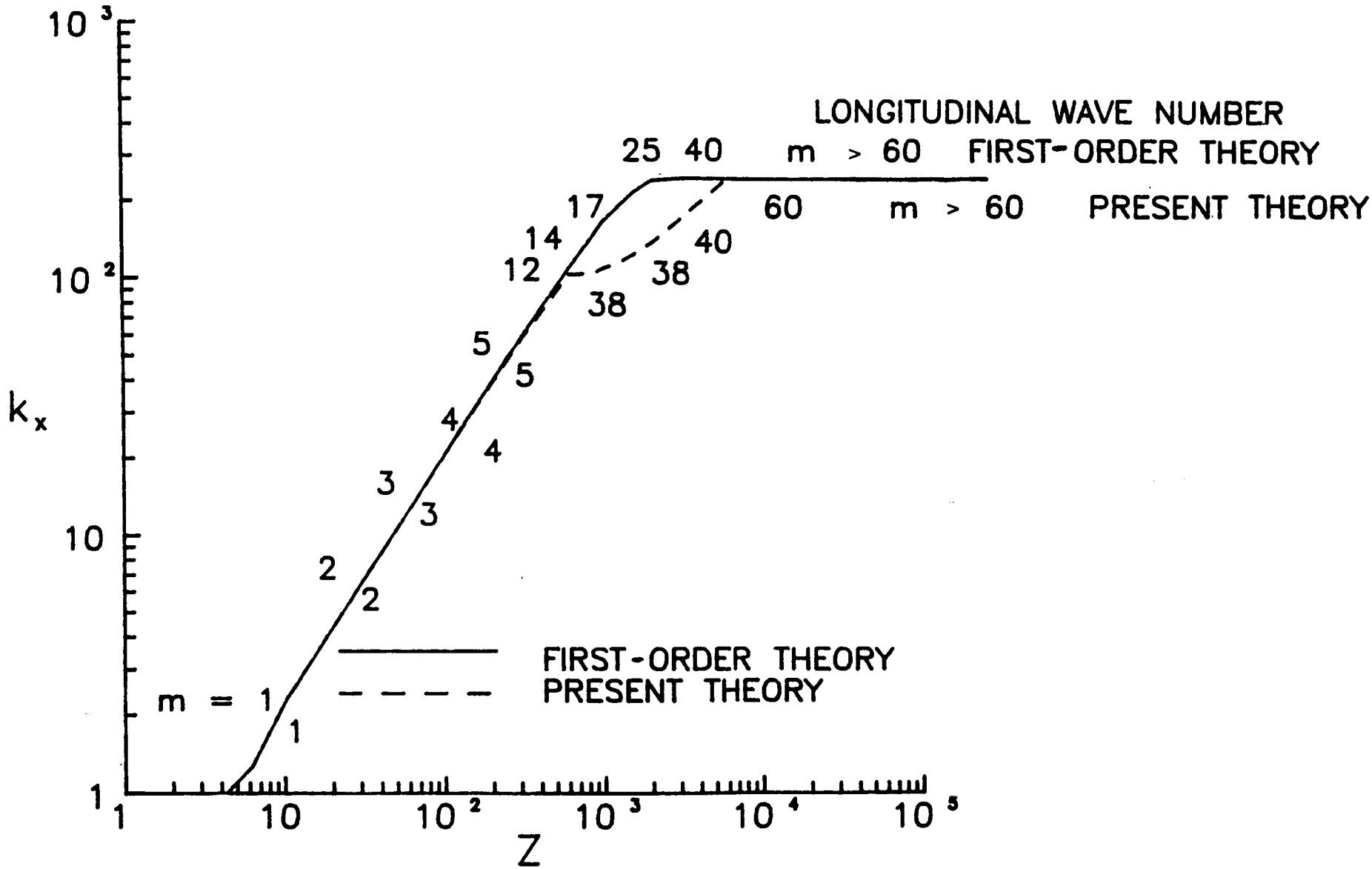

Figure 5. Change in mode shape of $[\pm 45/90]_{ns}$ laminated cylinders when transverse shear deformation is accounted for more accurately.

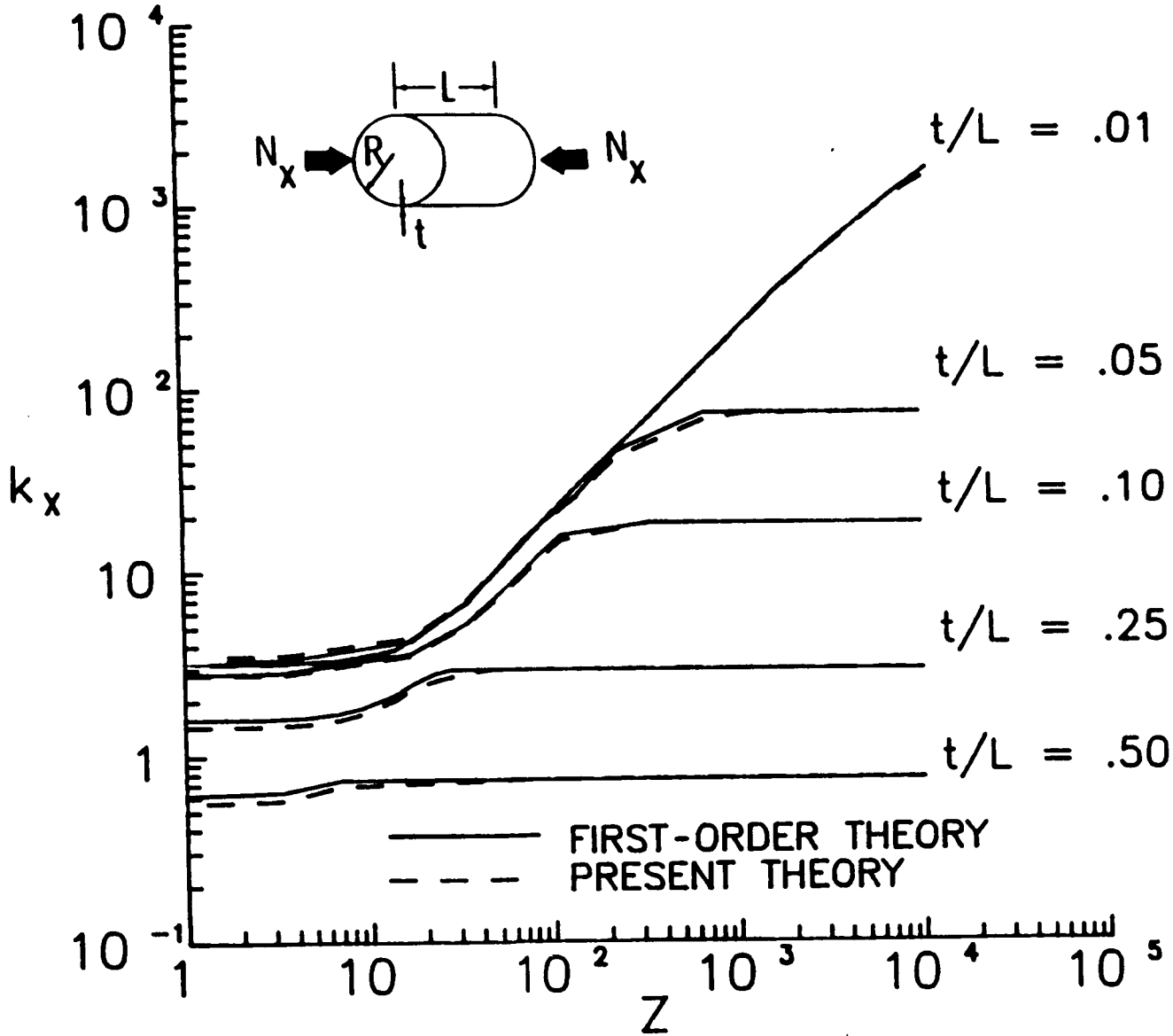

Figure 6. Effect of transverse shear deformation on axial compressive buckling loads of $[0]_{ns}$ laminated cylinders.

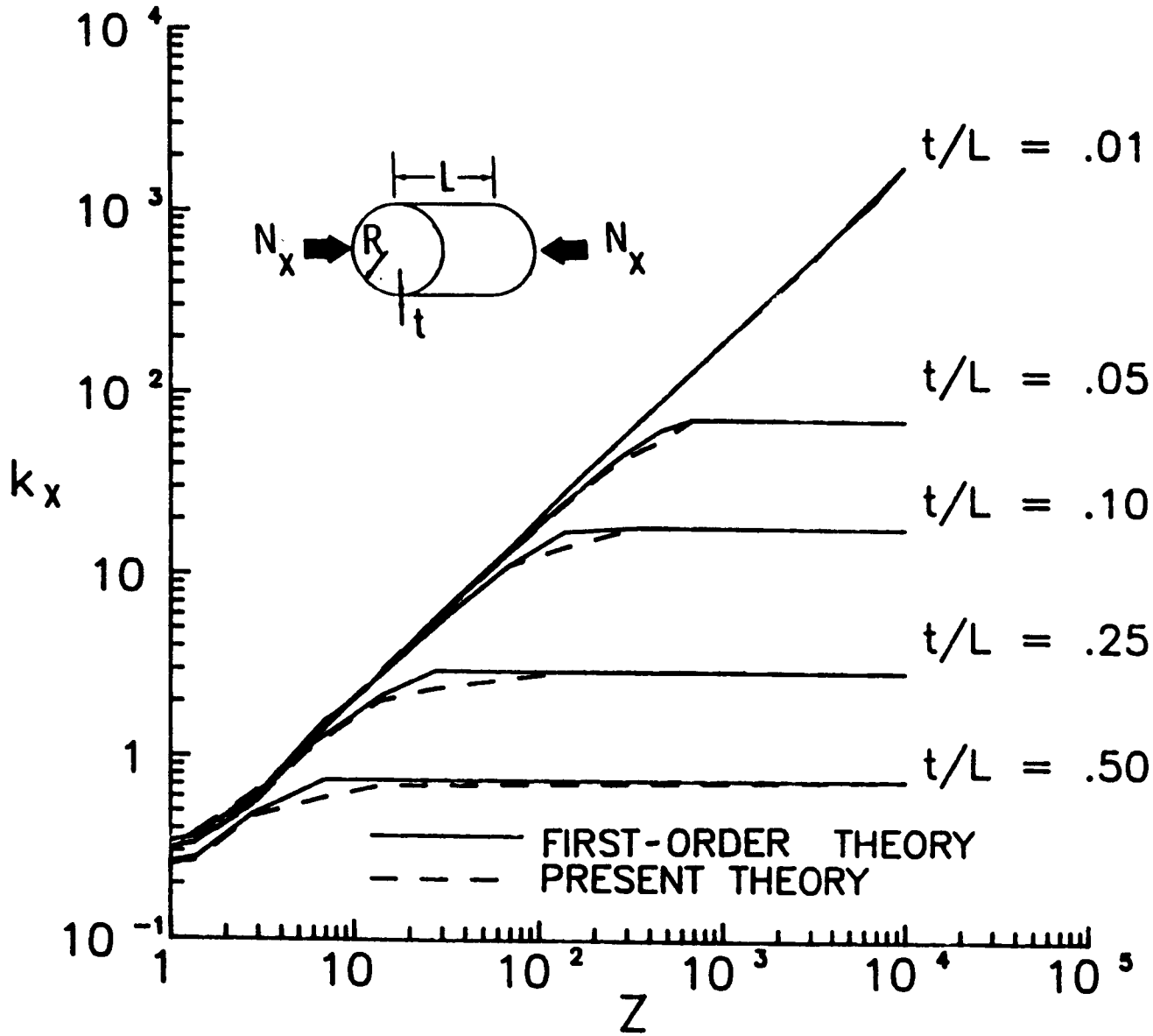

Figure 7. Effect of transverse shear deformation on axial compressive buckling loads of $[90]_{ns}$ laminated cylinders.

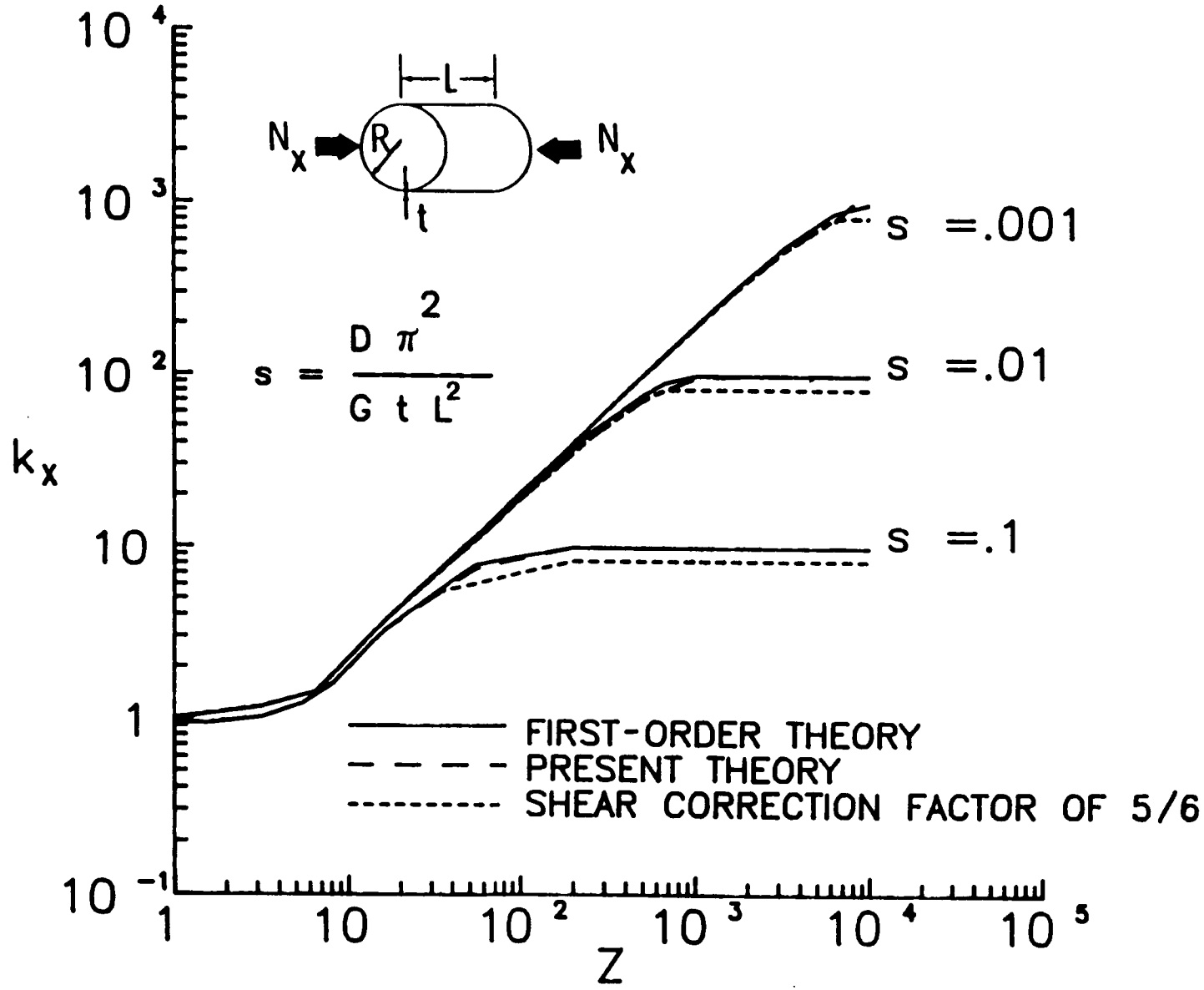

Figure 8. Comparison of buckling loads predicted by the present theory and by the first-order theory with a shear correction factor for isotropic cylinders.

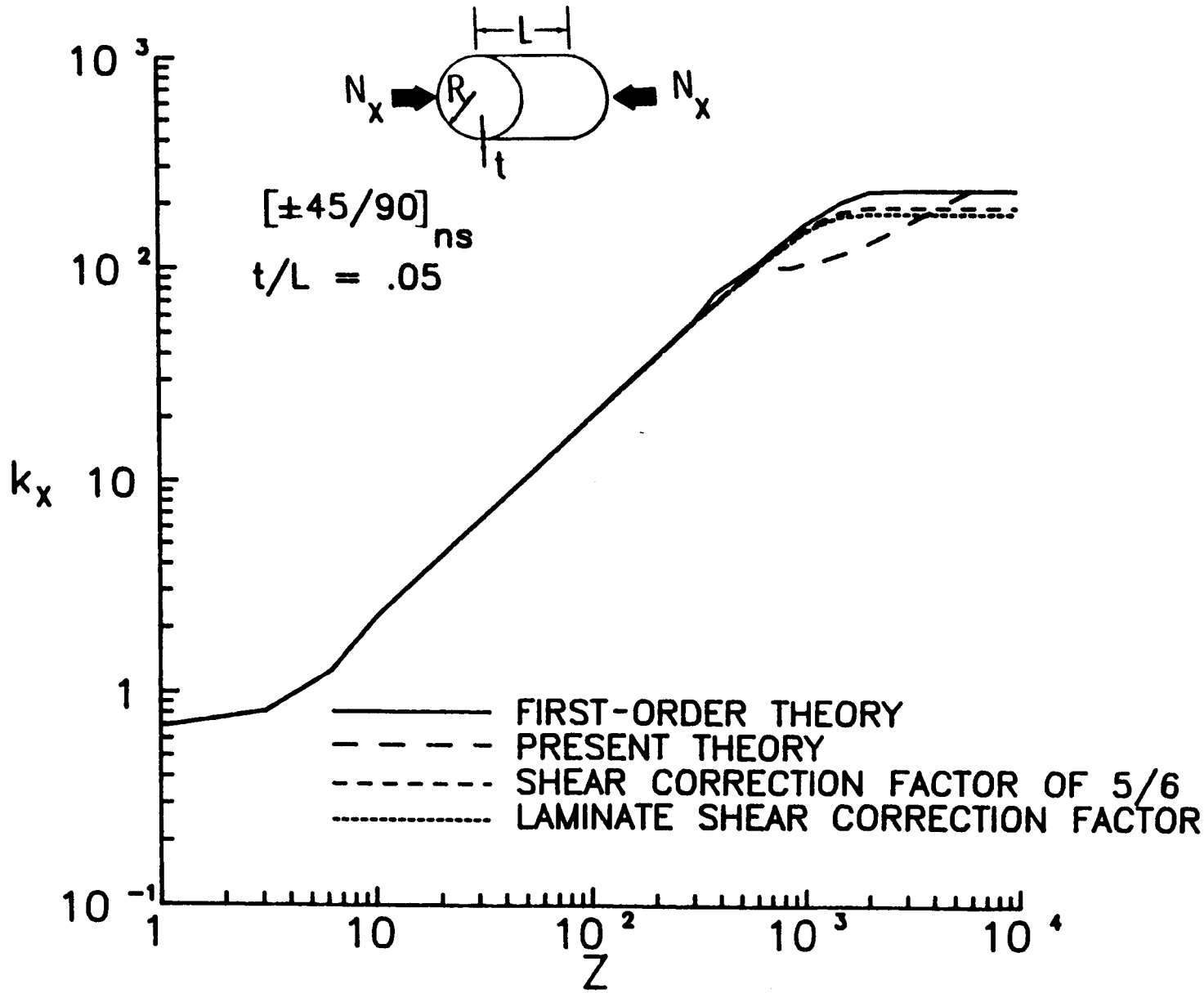

Figure 9. Comparison of buckling loads predicted by the present theory and by the first-order theory with shear correction factors for $[\pm 45/90]_{ns}$ laminated cylinders

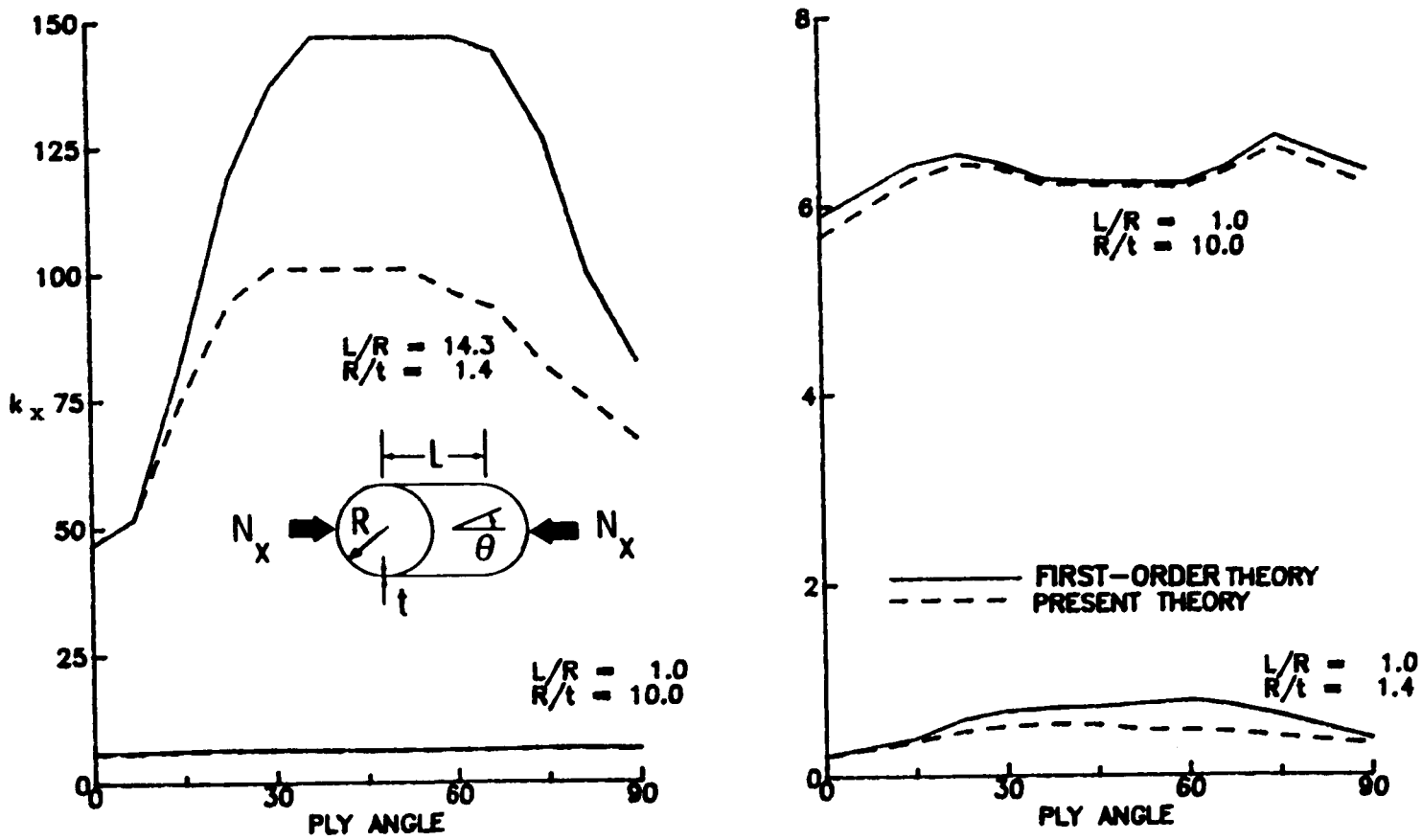

Figure 10. Effect of stacking sequence on axial compressive buckling load of $[\pm\theta/90]_{ns}$ laminated cylinders.

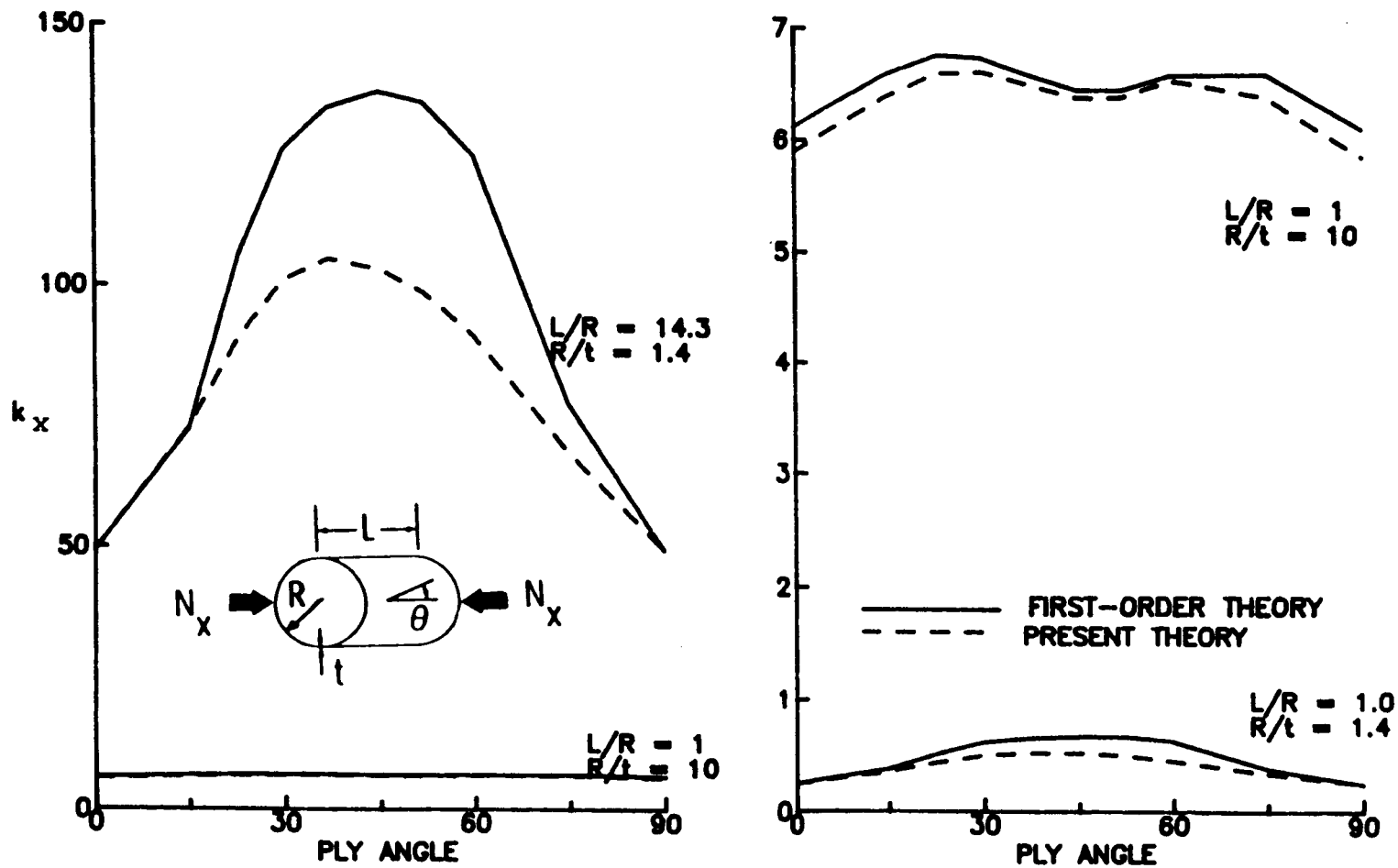

Figure 11. Effect of stacking sequence on axial compressive buckling load of $[\pm\theta/0/90]_{ns}$ laminated cylinders

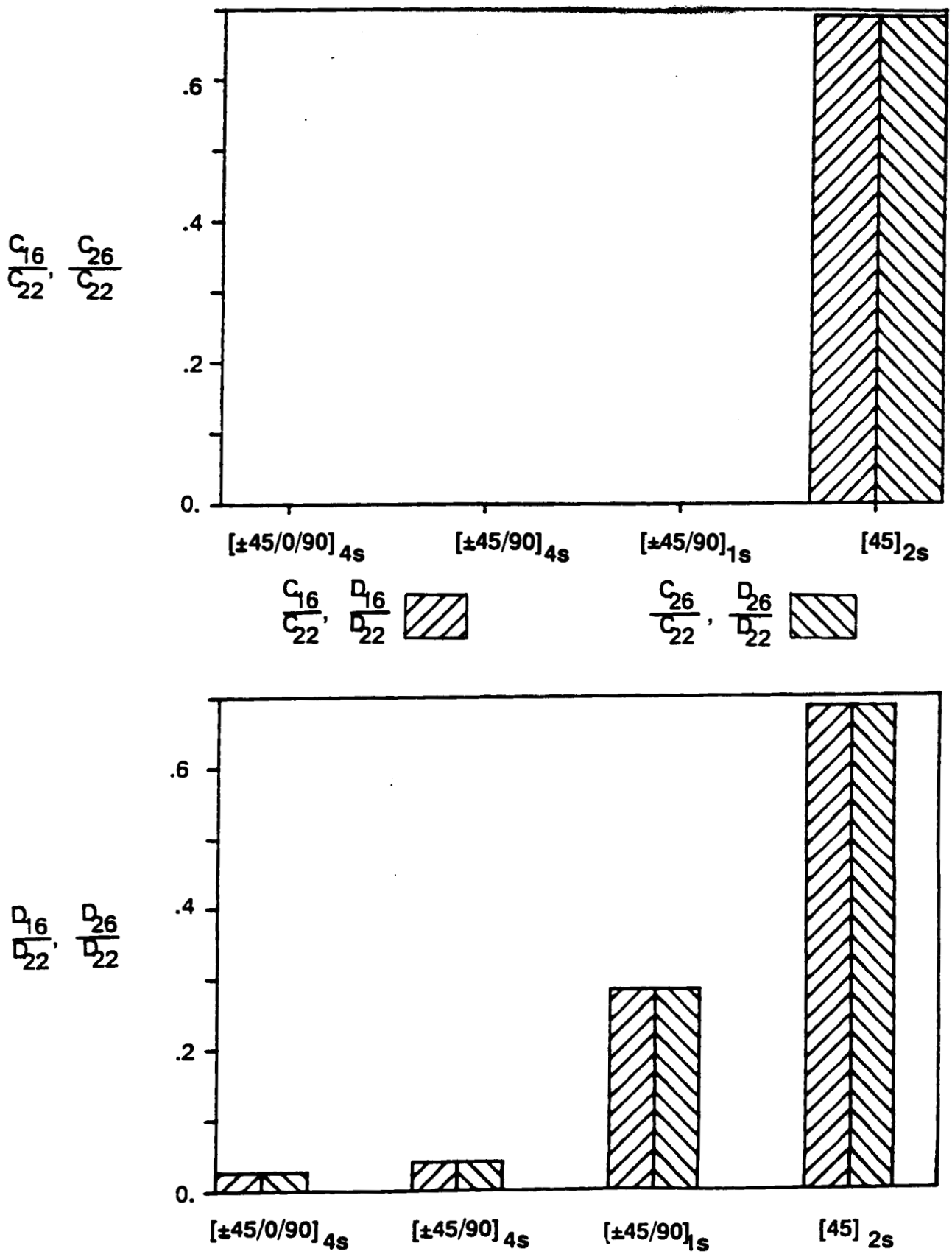

Figure 12. Anisotropic material properties of graphite-epoxy laminates.

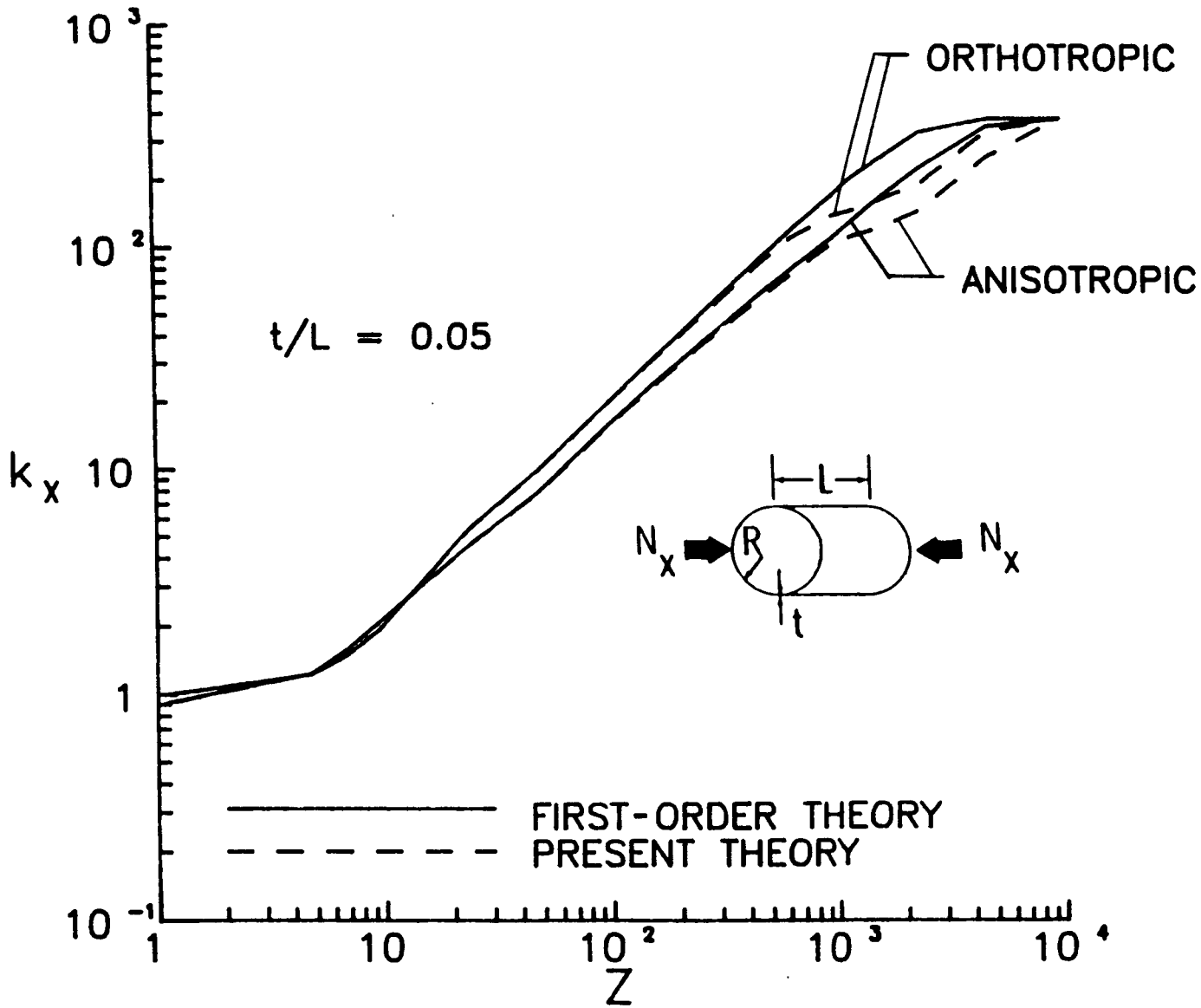

Figure 13. Buckling load of anisotropic $[45]_{ns}$ laminated cylinder predicted by assuming orthotropy and by assuming anisotropy.

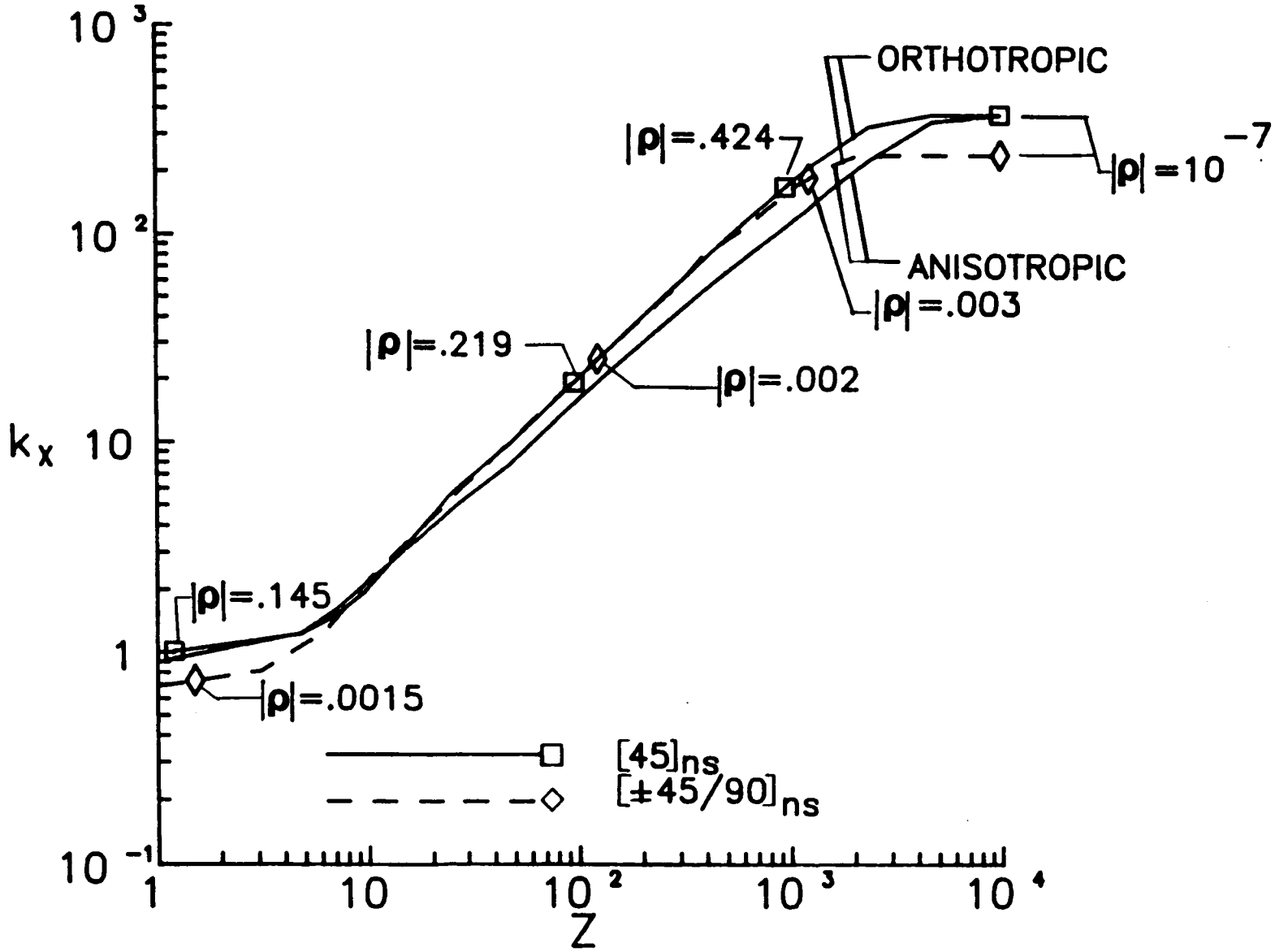

Figure 14. Sensitivity of $[45]_{ns}$ laminated cylinder to anisotropy.

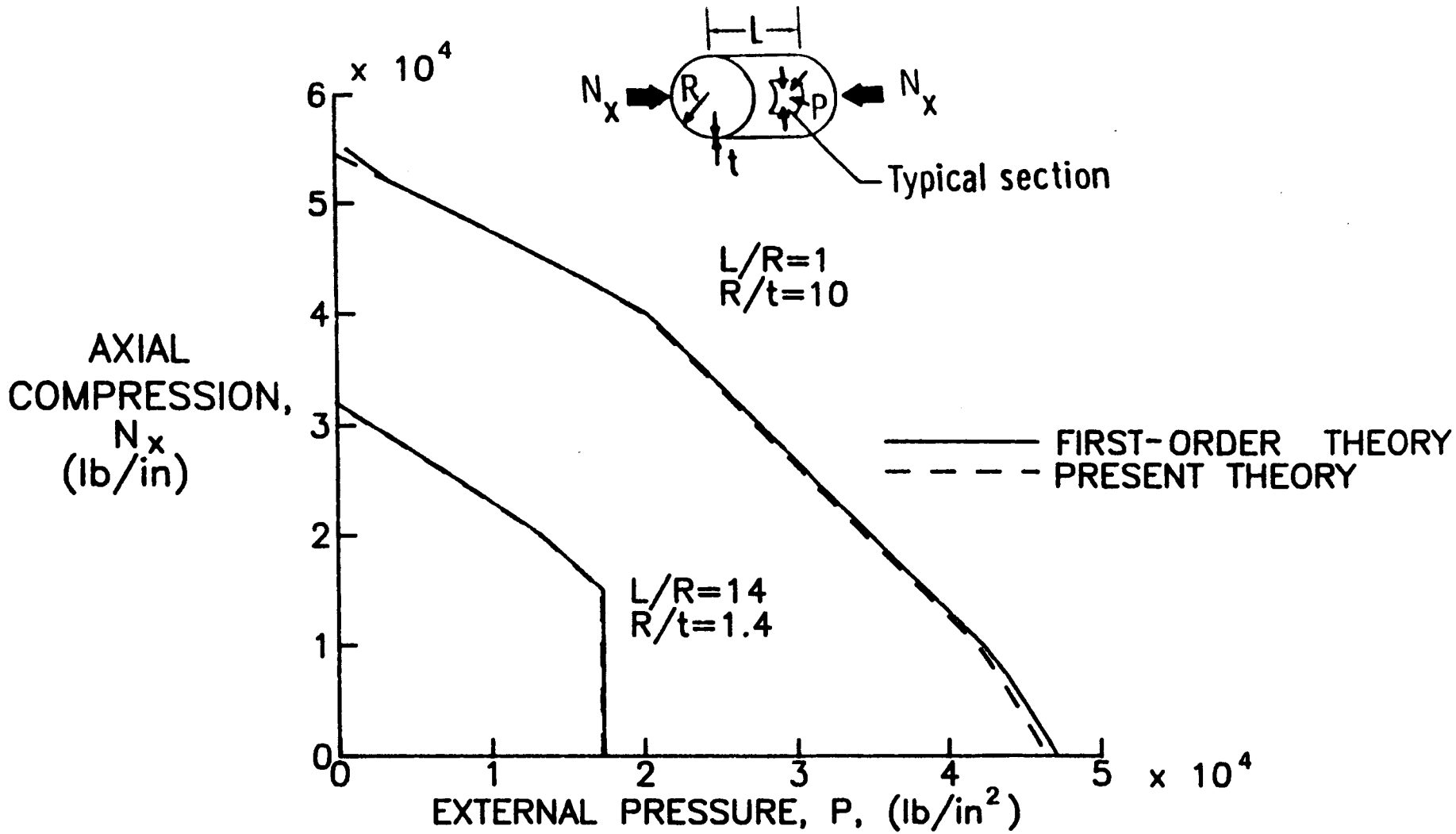

Figure 15. Interaction of axial compressive and external pressure loadings on buckling of isotropic cylinders.

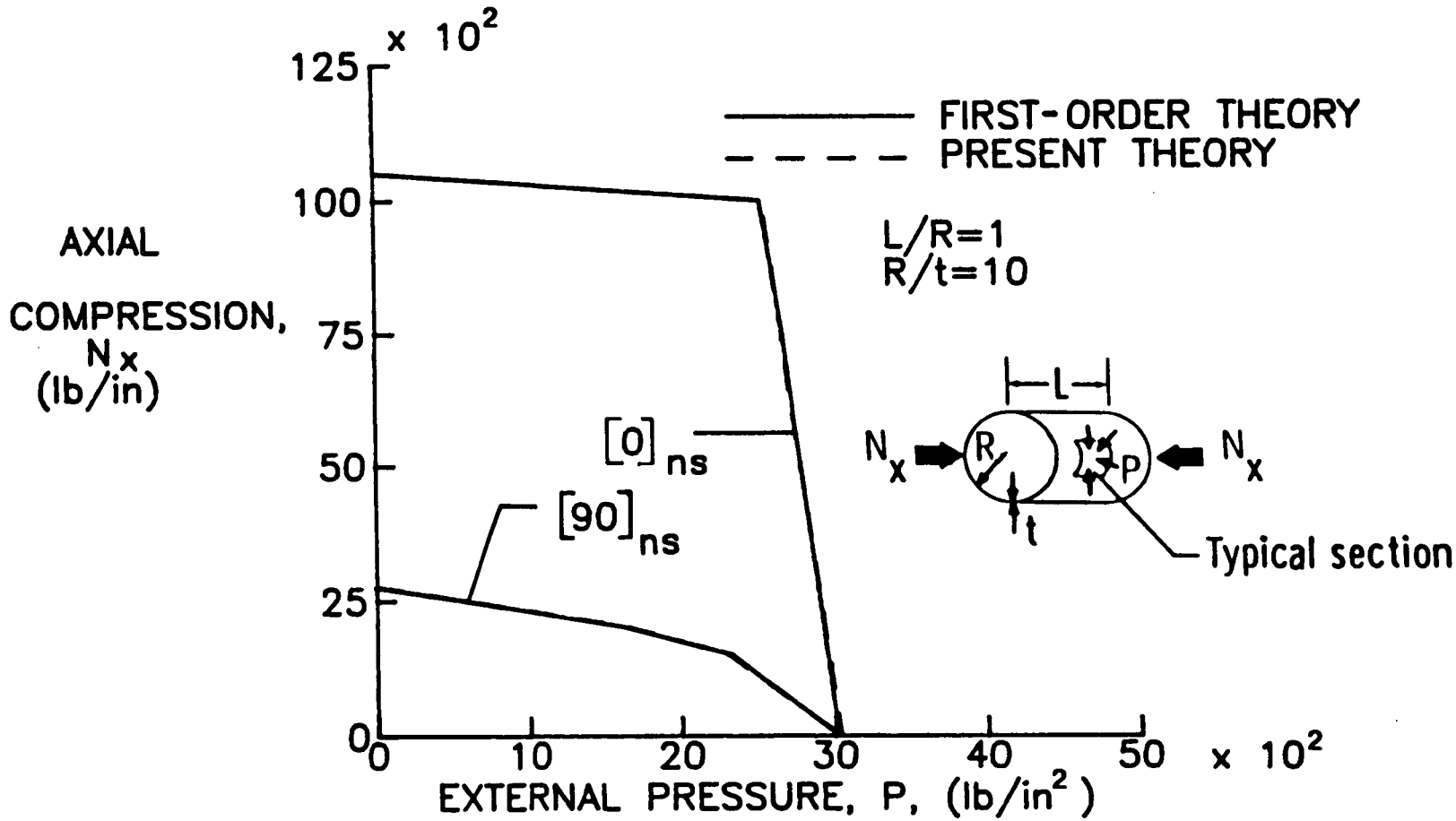

Figure 16. Interaction of axial compressive and external pressure loadings on buckling of laminated $[0]_{ns}$ and $[90]_{ns}$ cylinders with R/t=10.

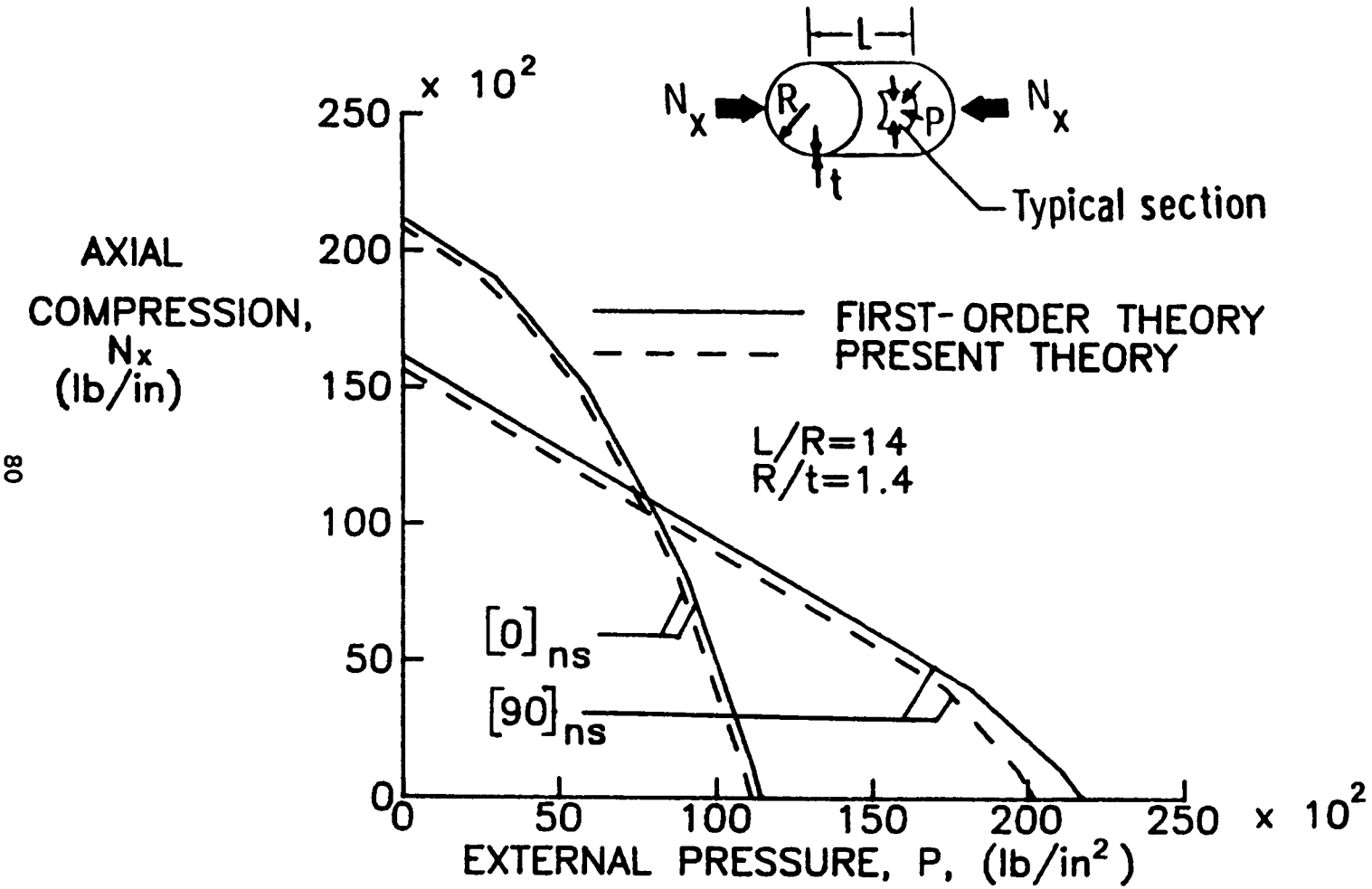

Figure 17. Interaction of axial compressive and external pressure loadings on buckling of laminated $[0]_{ns}$ and $[90]_{ns}$ cylinders with R/t=1.4.

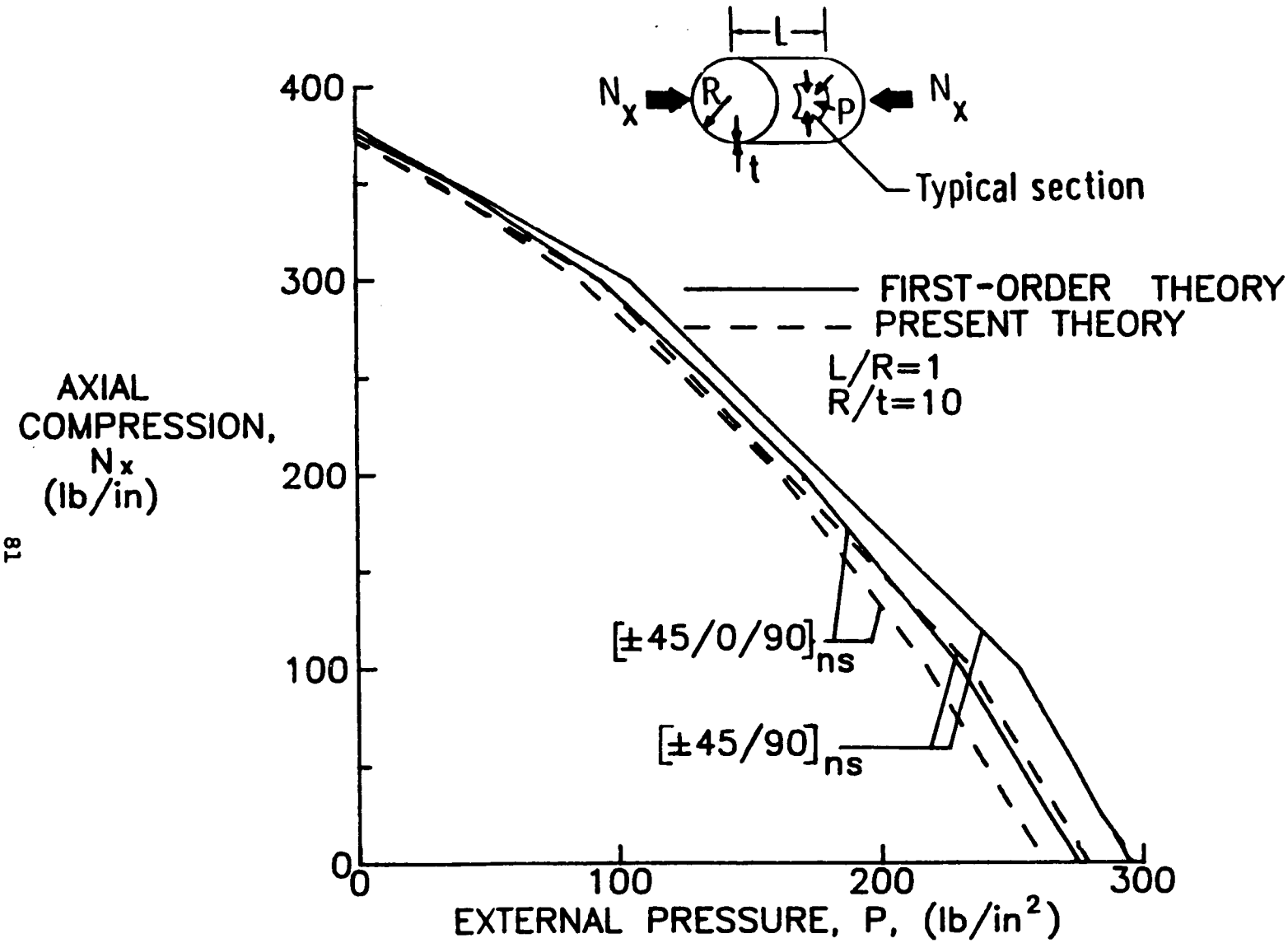

Figure 18. Interaction of axial compressive and external pressure loadings on buckling of laminated $[\pm 45/0/90]_{ns}$ and $[\pm 45/90]_{ns}$ cylinders with R/t=10.

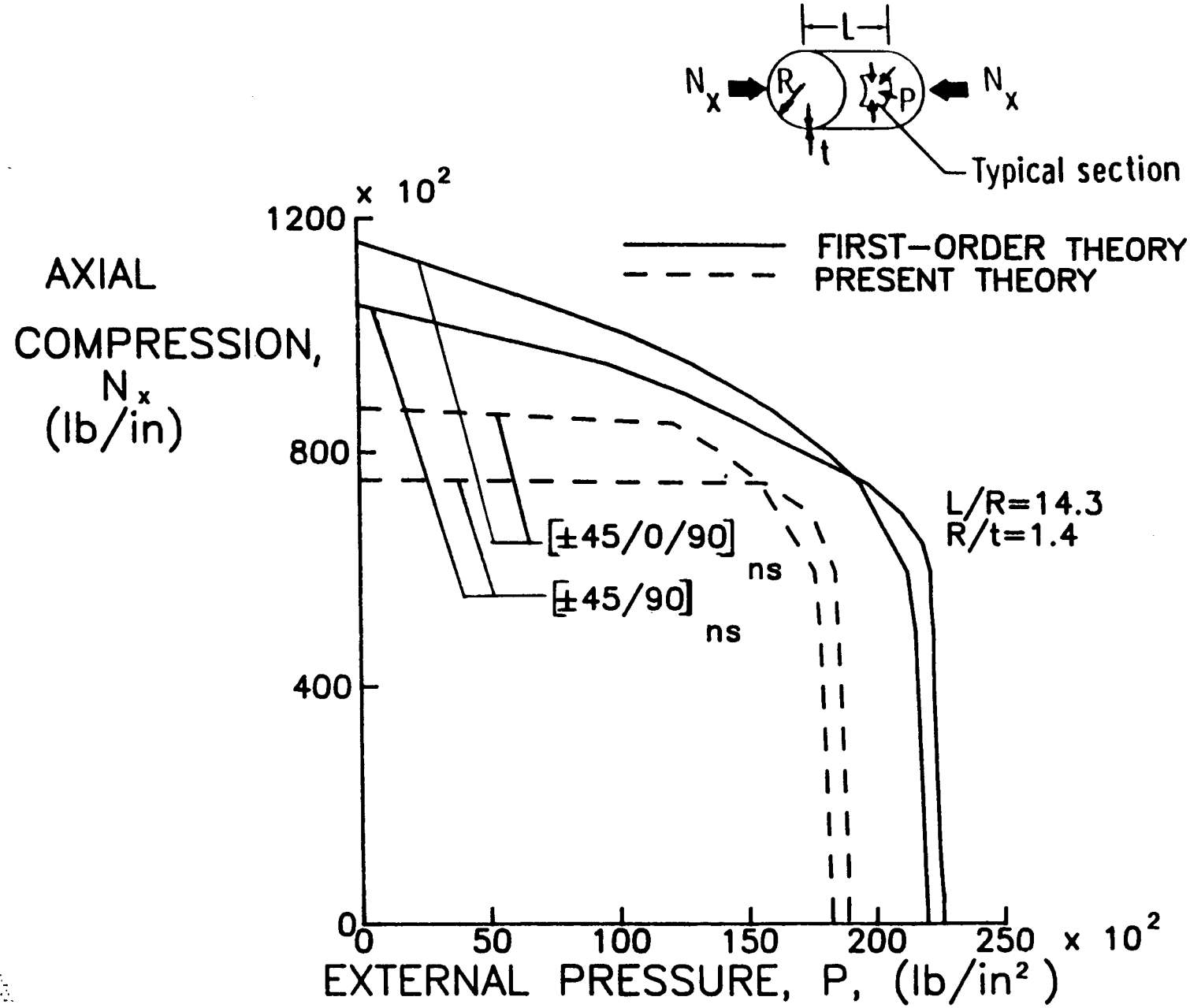

Figure 19. Interaction of axial compressive and external pressure loadings on buckling of laminated $[\pm 45/90/0]_{ns}$ and $[\pm 45/90]_{ns}$ cylinders with R/t=1.4.

NASA
National Aeronautics and Space Administration

Report Documentation Page

1. Report No.	2. Government Accession No.	3. Recipient's Catalog No.
NASA TM-100508		

4. Title and Subtitle	5. Report Date
An Analytical Study of the Effects of Transverse Shear Deformation and Anisotropy on Buckling Loads of Laminated Cylinders	October 1987
	6. Performing Organization Code
7. Author(s)	8. Performing Organization Report No.
Dawn C. Jegley	
	10. Work Unit No.
9. Performing Organization Name and Address	505-63-01-09
NASA Langley Research Center Hampton, VA 23665-2552	11. Contract or Grant No.
	13. Type of Report and Period Covered
12. Sponsoring Agency Name and Address	Technical Memorandum
National Aeronautics and Space Administration Washington, DC 20546	14. Sponsoring Agency Code

15. Supplementary Notes

Author's M.S. Thesis, George Washington University, Washington, DC.

16. Abstract Buckling loads of thick-walled orthotropic and anisotropic simply supported circular cylinders are predicted using a higher-order transverse-shear deformation theory. A comparison of buckling loads predicted by the conventional first-order transverse-shear deformation theory and the higher-order theory show that the additional allowance for transverse shear deformation has a negligible effect on the predicted buckling loads of medium-thick metallic isotropic cylinders. However, the higher-order theory predicts buckling loads which are significantly lower than those predicted by the first-order transverse-shear deformation theory for certain short, thick-walled cylinders which have low through-the-thickness shear moduli. A parametric study of the effects of ply orientation on the buckling load of axially compressed cylinders indicates that laminates containing 45-degree plies are most sensitive to transverse-shear deformation effects. Interaction curves for buckling loads of cylinders subjected to axial compressive and external pressure loadings indicate that buckling loads due to external pressure loadings are as sensitive to transverse-shear deformation effects as buckling loads due to axial compressive loadings. The effects of anisotropy are important over a much wider range of cylinder geometries than the effects of transverse shear deformation.

17. Key Words (Suggested by Author(s))	18. Distribution Statement
Transverse Shear Deformation Anisotrophy Buckling Loads Laminated Cylinders	Unclassified - Unlimited Subject Category - 24

19. Security Classif. (of this report)	20. Security Classif. (of this page)	21. No. of pages	22. Price
Unclassified	Unclassified	89	A05

NASA FORM 1626 OCT 86